

1-4-93

43PP

Contains No CBI

May 26, 1993



FYI-93-000893  
INIT 06/03/93

Document Control Officer  
Chemical Information Division  
Office of Toxic Substances (WH-557)  
Environmental Protection Agency  
401 M Street, S.W.  
Washington, D.C. 20460



8493000031

To Whom It May Concern:

A

06 JUN 11 11:30

The following report is being sent to you on an F.Y.I. basis.

A study of the *in vitro* toxicology of diatomaceous earth (DE) products has been completed at Mountain Technical Center (MTC) of Schuller International, Inc. Findings are summarized below; complete report is attached.

At this time, there are no known *in vitro* tests that have been validated to predict the pathogenic potential of respirable dusts to the whole organism. It is not known to what, if any, extent the results from *in vitro* tests reflect what happens in the whole organism.

*In Vitro* toxic effects of four siliceous dusts were evaluated in cultures of Chinese hamster ovary (CHO) cells using four toxic endpoints: inhibition of proliferation, colony forming efficiency, cell viability as measured by intracellular esterase activity, and micronucleus induction. Natural and flux-calcined (heated to >2000°F with soda ash; decreases surface area by melting and closing smaller porosities) diatomaceous earth (DE) products were size-separated to provide two respirable subpopulations of the bulk product. These two respirable subpopulations were used as the test dusts for the *in vitro* studies; they are designated Nat and FC, respectively. Toxic effects of Nat and FC were compared with those of two pure crystalline silica reference dusts,  $\alpha$ -quartz and cristobalite, as well as TiO<sub>2</sub> and UICC crocidolite asbestos (CD). All four silica dusts elicited a qualitatively similar, concentration-dependent response pattern in the CHO cells, consisting of particle uptake, visible nuclear alterations (micro-, multiple-, and/or misshapen nuclei), reduction in

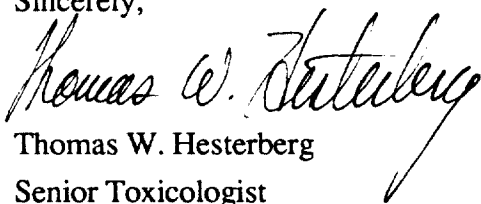
Mountain Technical Center  
10100 West Ute Avenue (80127)  
P.O. Box 625005  
Littleton, CO 80162-5005  
Tel 303 978-5200

RECEIVED  
12-9-93

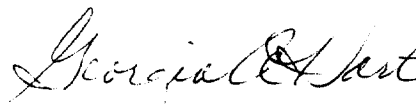
SCHULLER  
A Unit of Schuller International, Inc.

cell proliferation and colony formation, and no evidence of decreased cell viability. This same pattern has been observed in CHO and other cultured cells exposed to crocidolite and other mineral and vitreous fibers. However, the severity of toxic response varied among the test particulates. When the EC50's (concentration which reduced cell proliferation to 50% of negative controls) of the 4 silica dusts were calculated as  $\mu\text{g}/\text{cm}^2$ , Nat was the most toxic ( $\text{EC}_{50} = 4 \mu\text{g}/\text{cm}^2$ ) and cristobalite was least toxic ( $\text{EC}_{50} = 25 \mu\text{g}/\text{cm}^2$ ). The ranking shifted when concentration was calculated as number of particles/ $\text{cm}^2$ : FC was the most toxic ( $\text{EC}_{50} = 860 \times 10^3$ ), Nat and cristobalite were similar ( $\text{EC}_{50} = \sim 2000 \times 10^3$ ), and  $\alpha$ -Quartz was least toxic ( $\text{EC}_{50} = 8400 \times 10^3$ ). In an attempt to determine the causes of these differences in toxicity, various parameters (crystallinity, surface area, particle dimensions, % fibrous particles) of the four dusts were compared. Natural DE is primarily amorphous while flux calcined DE is 40% crystalline and the two reference dusts are >96% crystalline. The number of particles/ $\mu\text{g}$  was 6.5-fold greater in Nat than in FC, and Nat was estimated to have a 10-fold greater surface area than FC. One possible cause of toxic differences could be a combination of surface area and surface chemistry resulting in different adsorbance capacities of the various particulates for cellular constituents. Another possible cause of toxic differences could be percentage of particles that are fibrous (length/diameter  $\geq 3$ ). When EC50's are calculated as number of fibers longer than 7.5  $\mu\text{m}$  per  $\text{cm}^2$ , the EC50's for Nat, FC, cristobalite and CD are very similar to each other (214, 259, 214 and 384, respectively,  $\times 10^3$ ).  $\alpha$ -quartz and  $\text{TiO}_2$  had no fibrous particles. Further investigations of DE materials are needed to test these hypotheses. A clarification of the relationships between toxicity and particle characteristics could provide a major step toward an understanding of the cellular mechanisms of particulate toxicology.

Sincerely,



Thomas W. Hesterberg  
Senior Toxicologist  
Health Safety and Environment



Georgia A. Hart  
Biologist

cc: R. Anderson, A. Jankousky, R. Versen, J. Chase, R. Batson, M. Merliss  
(International Diatomaceous Earth Producers Assoc.), M. Fleischman (Celite Corp.), V.  
Vu (US EPA)

**Contains No CBI**

**In Vitro Toxicology of  
Size-Selected Fractions of  
Diatomaceous Earth  
Products**

**G. A. Hart and T. W. Hesterberg**

**May 1993**

**Mountain Technical Center, Schuller Int.**

**In Vitro Toxicology Laboratory**

**Littleton, Colorado**

CONFIDENTIAL

# In Vitro Toxicology of Size-Selected Fractions of Diatomaceous Earth Products

## Table of Contents

	Page No.
<b>Abstract</b>	1
<b>I. Introduction</b>	2
<b>II. Test Particulates</b>	4
Rationale for Selection of Test Articles	4
Preparation and Characterization	5
<b>III. Methods and Materials</b>	7
In Vitro Assays	7
Cell Proliferation Assays	7
Viability Assays	7
Nuclear Abnormality Assay	8
Inhibition of Proliferation with Leachates vs. Particulates	9
Test System, CHO-K1 Cell Line	10
<b>IV. Results</b>	11
<b>V. Discussion and Recommendations</b>	15
<b>VI. References</b>	18
<b>VII. Acknowledgements</b>	19
<b>VIII. Figures</b>	
1. SEM Micrographs of Test Articles, A-H.	
2. Particle Lengths	
3. Inhibition of Cell Proliferation, CHO-K1 Cells	
4. Colony Forming Efficiency, CHO-K1 Cells	
5. Inhibition of Cell Proliferation, Particles v. Filtered, Particle-Exposed Medium	
6. Esterase Activity Viability after 1, 2, and 3 Days Exposure	
7. Inhibition of Cell Proliferation after 1, 2, and 3 Days Exposure	
8. Induction of Nuclear Abnormalities	
9. Photomicrographs of CHO-K1 Cells Growing in Culture Medium	
10. Photomicrographs of CHO-K1 Cells Exposed to s-Nat DE	
11. Photomicrographs of CHO-K1 Cells Exposed to s-FC DE	
12. Photomicrographs of CHO-K1 Cells Exposed to Cristobalite	
13. Photomicrographs of CHO-K1 Cells Exposed to alpha-Quartz	
14. Photomicrographs of CHO-K1 Cells Exposed to UICC Crocidolite Asbestos	
<b>IX. Tables</b>	
I. Test Articles, Bulk Materials	
II. Comparison of Effective Concentration-50, EC 50	
<b>X. Appendices</b>	
1. Test Particulates, Average Dimensions	
2. Particle Dimensions	
3. In Vitro Tests	
4. Esterase Activity Viability Data	
5. Induction of Nuclear Abnormalities Data	

# **In Vitro Toxicology of Size-Selected Fractions of Diatomaceous Earth Products**

G.A. Hart and T.W. Hesterberg  
Mountain Technical Center, Schuller International, Littleton, Colorado

## **ABSTRACT**

In Vitro toxic effects of four silicon dusts were evaluated in cultures of Chinese hamster ovary cells (CHO) using four toxic endpoints: inhibition of proliferation, colony forming efficiency, viability as measured by intracellular esterase activity, and micronucleus induction. Natural and flux-calcined diatomaceous earth (DE) products were size-separated to provide two respirable test dusts, Nat and FC, respectively. Toxic effects of the two diatomaceous earth dusts were compared with those of two pure crystalline silica reference dusts (α-quartz and cristobalite), TiO<sub>2</sub> and UICC crocidolite asbestos (CD). All four silica dusts elicited a similar, concentration-dependent response pattern in the CHO cells, consisting of particle uptake, visible nuclear alterations (micro-, multiple-, and/or misshapen nuclei), reduction in cell proliferation and colony formation, and no evidence of decreased cell viability. This same pattern has been observed in CHO and other cell cultures exposed to crocidolite and other mineral fibers. However, the severity of toxic response varied among the test particulates. When the EC<sub>50</sub>'s (concentration which reduced proliferation to 50% of negative controls) of the 4 silica dusts were calculated as μg/cm<sup>2</sup>, Nat was the most toxic (EC<sub>50</sub> = 4 μg/cm<sup>2</sup>) and cristobalite was least toxic (EC<sub>50</sub> = 25 μg/cm<sup>2</sup>). The ranking shifted when concentration was calculated as number of particles/cm<sup>2</sup> -- FC was the most toxic (EC<sub>50</sub> = 860 × 10<sup>3</sup>), Nat and cristobalite were similar (EC<sub>50</sub> = ~2000 × 10<sup>3</sup>), and α-Quartz was least toxic (EC<sub>50</sub> = 8400 × 10<sup>3</sup>). In an attempt to determine the causes of these differences in toxicity, various parameters (crystallinity, surface area, particle dimensions, % fibrous particles) of the four dusts were compared. Natural DE is primarily amorphous while flux calcined DE is 40% crystalline and the two reference dusts are >96% crystalline. The number of particles/μg was 6.5-fold greater in Nat than in FC, and Nat was estimated to have a 10-fold greater surface area than FC. One possible cause of toxic differences could be a combination of surface area and surface chemistry resulting in different adsorbencies of the various particulates for cellular constituents. Another possible cause of toxic differences could be percentage of particles that are fibrous (length/diameter ≥ 3). When EC<sub>50</sub>'s are calculated as number of fibers longer than 7.5 μm per cm<sup>2</sup>, the EC<sub>50</sub>'s for Nat, FC, cristobalite and CD are very similar to each other (214, 259, 214 and 384, respectively, × 10<sup>3</sup>). α-quartz and TiO<sub>2</sub> had no fibrous particles. Further investigations of DE materials are needed to test these hypotheses. A clarification of the relationships between toxicity and particle characteristic could provide a major step toward an understanding of the cellular mechanisms of particulate toxicology.

## INTRODUCTION

In vitro cytotoxicity of particulates has in some cases paralleled in vivo pathogenesis (Hart et al., 1992). However, the in vitro responses of cells to a toxin may vary greatly depending upon the cell type and the species of origin. Therefore, no single in vitro test system has been demonstrated to predict the toxicity of a substance in the whole animal. Furthermore, some in vivo correlates of particulate toxicity cannot at this time be measured in vitro, such as lung deposition and clearance and long term biopersistence. Therefore, a battery of in vitro tests is recommended as a means of screening materials for their toxicologic potential, followed by short term animal inhalation studies to determine lung deposition and clearance, and finally long term animal inhalation studies to determine biopersistence and pathogenesis (Hesterberg et al., 1991).

The purpose of the present study was to develop data which might contribute to a better understanding of the cellular mechanisms of particulate toxicity. To this end, the study utilized size-selected, respirable diatomite subfractions which were well characterized in terms of particle number/ $\mu\text{g}$ , size, shape and crystallinity. These subfractions should be further characterized for surface area and chemical composition.

The in vitro systems herein described utilized four different assays, each of which measures a different parameter of toxicity: cell proliferation, viability, colony forming efficiency and abnormal nucleus induction (methods described in *Appendix*). In vitro cell responses to size-selected sub-fractions of two diatomite types (natural and flux calcined) were compared with responses to two reference chemicals (cristobalite and  $\alpha$ -quartz), all of which were composed of particles within the respirable range. Two tests also included titanium dioxide particles, which is generally considered to be a nontoxic, nuisance dust.

In these assays, the in vitro toxicity of size-selected diatomites is quantitatively similar to that of crocidolite asbestos. DE also induced abnormal nuclei that were similar to those induced by CD and other vitreous fibers (Hart et al., 1992a, 1992b); however, some qualitative differences were noted between DE-induced and fiber-induced abnormalities, respectively (see *Results*). In contrast to the diatomites, the in vitro toxicity of the two reference crystalline silica particulates (cristobalite and quartz) was relatively low and similar to that observed with titanium dioxide.

Suggestions for follow-up in vitro research include the use of lung cell types derived from the actual target tissues of particle-induced respiratory disease in humans and animals (lung epithelium, macrophages, mesothelium and/or fibroblasts). To determine the particle characteristics that are responsible for the toxic effects, assays could be conducted using an assortment of different DE dusts that have been altered in various ways, e.g., particle size and shape, total surface area, and chemical composition (see *Discussion*).

## TEST PARTICULATES

### Selection of Test Particles, Rationale

Natural and flux calcined diatomaceous earth (DE) were obtained from Celite Corporation and subjected to a size-separation process in the MTC Particle Preparation Laboratory (see next section). These two diatomite forms have some similarities as well as important differences (Table I.). Both are composed of fine, porous silicon dioxide particles in a variety of sizes and shapes (see photographs, Figure 1A-H.)). The Materials Safety and Data Sheets (MSDS) provided by Celite for these two products show a major difference in crystallinity. Natural DE is mostly amorphous silica, with less than 3% crystalline quartz. Flux calcined DE has a much higher crystalline content; it also contains no more than 3% quartz but can be as much as 60% cristobalite (Table I). This agrees with the crystallinity analysis performed on the bulk products at MTC: natural DE had 3.98% quartz and no cristobalite; flux calcined DE had 1.95% quartz and 39.59% cristobalite.

Other differences between the two forms of DE that could influence toxicity could exist in surface area, porosity, density, size, shape and surface chemistry. Surface area in bulk natural DE is 10- to 20-fold greater (roughly 20 cubic meters/gram) than in flux calcined (approximately 1-2 cubic meters/gram). Porosity is generally believed to be less prevalent and finer in flux calcined than in natural DE (verbal communication, Garth Coombs, Schuller Int., Inc.). Density (number of particles/unit mass), size and shape were evaluated for the size-selected test particles (Table II.) and are discussed in *Results*. Surface chemistry was not analyzed in the present study.

The alpha-quartz and cristobalite particles used in this study are respirable reference chemicals from the U.S. National Bureau of Standards (NBS). These two particulates are

two different, pure crystalline forms of silicon dioxide (96% and 98% purity, respectively). Quartz and cristobalite were selected for use in the study in order to evaluate the toxic impact of crystalline versus amorphous silicon dioxide.

The toxic effects of DE are compared with the toxicity of Union Internationale Contre Cancer (UICC) crocidolite asbestos (CD), which was evaluated in the MTC In Vitro Laboratory in a separate study. CD was obtained from V. Timbrell\*. Titanium Dioxide was obtained from the U.S. National Bureau of Standards, Standard Reference No. 154a.

### **Test Article Preparation and Characterization**

Natural diatomite and flux calcined diatomite products were subjected to a size-selection process at MTC to provide a test material of each that is composed of particulates within the respirable size range. The size-selected fractions of these two materials are designated S-Nat and S-FC. CD and the three reference chemicals, cristobalite, alpha-quartz and titanium dioxide, were not size-selected because they were in the respirable size range as supplied.

Because particle size and geometry are known to be critical determinants of toxicity, especially with fibrous materials, length, width and aspect ratio (length/width) were determined for each of the test articles using scanning electron microscopy (SEM). Length and width were determined for each of 100 particles by measuring first the longest axis and then the perpendicular axis that appeared to be representative of the width of the particle. Data are summarized in Table II and graphed in Figure 2. S-Nat and S-FC are composed of particles in a variety of shapes and sizes, some of which (38% and 36%, respectively) are more or less fibrous (fibrous is here defined as having an aspect ratio  $\geq 3$ ). In Figure

---

\* Dr. V. Timbrell, Pneumoconiosis Research Unit, Llandough Hospital, Penarth, Glamorgan, U.K.

1, it can be seen that S-Nat has a population of particles that are similar in size to those of S-FC, but the former also contains a second population of particles that are much smaller than those of the latter. Average dimensions of the constituent particles of natural DE are  $3.8 \pm 3.9 \mu\text{m} \times 1.3 \pm 1.0 \mu\text{m}$  and of flux calcined DE are  $5.9 \pm 4.1 \mu\text{m} \times 2.1 \pm 1.5 \mu\text{m}$ . Cristobalite particles fall roughly in the size ranges of the diatomites and a portion (21%) of these are fibrous (aspect ratio  $\geq 3$ ), while alpha-quartz particles are much smaller and do not have a significant portion of fibrous shapes. Figure 1 also includes an electron micrograph of titanium dioxide particles at approximately 1000X.

The toxicity of fibers may be influenced more by particle number than by particle mass Hart et al., 1992a and 1992b). The same may be true for non-fibrous particulates. Therefore the number of particles/ $\mu\text{g}$  was determined for each of the test articles (Table II). Note that the number of particles/ $\mu\text{g}$  is roughly eight times greater for S-Nat and quartz (514,000 and 525,000 particles/ $\mu\text{g}$ , respectively) than for S-FC and cristobalite (78,000 and 75,000 particles/ $\mu\text{g}$ , respectively), Table II. The higher number of particles/ $\mu\text{g}$  in S-Nat and quartz could be related to smaller average particle sizes, particularly the smaller diameters of these two materials (1.3 and 1.1  $\mu\text{m}$ , respectively). Differences in porosity may also play a role in that flux calcined DE particles may be less porous and therefore heavier, resulting in fewer particles per unit mass. Differences in porosity would also result in differences in surface area, which could in turn impact toxic effect if surface chemistry is involved in toxicity (e.g., adsorption and subsequent disruption of cellular components). Future studies should determine the surface area of the size-selected particulates as well as the bulk starting material. Surface chemistry should also be analyzed.

## METHODS AND MATERIALS

The four assays used to assess the in vitro cytotoxicity of the test articles are described below. Methodologies are summarized in the *Appendix*.

### Cell Proliferation Assays

Two different assays were used to measure the potential of the test material to inhibit cell proliferation: the "Inhibition of Cell Proliferation" (ICP) and the "Colony Forming Efficiency" (CFE) assay. Each test included 3-4 concentrations of each test material, negative controls of cells in growth medium only, and 3 replicates of each exposure. Each of the two assays was conducted a minimum of three times. These two assays do not distinguish between the cessation of cell division and the outright killing of cells.

### Cell Viability Assay

The esterase activity viability (EAV) assay was utilized to assess cell viability. Cultures of CHO-K1 cells were exposed to a high concentration of the test article for three days and harvested as described for the ICP assay. Suspensions of the harvested cells were treated with carboxyfluorescein (CF), a non-fluorescent ester, which is taken up by both viable and non-viable cells. The intracellular CF is cleaved by cytoplasmic esterases and then becomes both polar and fluorescent. The polar compound accumulates in the viable cells because the intact membranes of healthy cells do not permit polar molecules to escape. The non-viable cells, with damaged membranes, lose the dye as rapidly as it forms and therefore do not fluoresce.

## **Nuclear Abnormality Assay**

The impact of the test articles on nuclear material was assessed by an assay which measures the induction of nuclear abnormalities (INA). This assay was developed from a standard genotoxicity assay which measures the incidence of micronucleus formation. A micronucleus is believed to form as a result of chemical or mechanical breakage of chromosomes or disturbance of chromosome migration during cell division. In previous cell culture studies with asbestos, small groups of chromosomes or chromosome fragments were displaced from the two masses of chromosomes which had migrated to the opposite poles of the dividing cell (Hesterberg and Barrett, 1985). These 'lost' chromosomes become incorporated in their own nuclear membrane and appear as a small, secondary nucleus alongside the main cell nucleus.

Micronucleus formation, with few other visible nuclear deformities, is typically induced in CHO cells as a result of treatment with a soluble chemical carcinogen such as mitomycin. However, in vitro exposure to certain particulates, such as asbestos and some other mineral fibers, induces a range of nuclear abnormalities, including micronuclei, multiple nuclei, and many-lobed nuclei. Other studies have shown a dose-dependent increase in structural and numerical chromosomal changes with increasing concentrations of asbestos or other mineral fibers (Sincock, et al., 1982). In our laboratory, the incidence of nuclear abnormalities increases with increasing CD concentration, suggesting that these abnormalities are related to chromosomal changes induced by the fibers. Therefore, the INA assay used in this study determines the incidence of all of the above nuclear abnormalities.

## **Inhibition of Proliferation with Particle-Exposed Medium versus Particulates**

Toxic effects observed following exposure to the test particles could be a result of one or more phenomena, including: (1) direct contact between particles and cells, in which particle size, shape and/or surface chemistry impacts cell structure; (2) removal of essential growth substances from the culture medium as a result of the adsorption of these substances onto the surface of the test particles; or (3) release of toxic chemicals into the growth medium as a result of test particle leaching. The second two possibilities were tested using proliferation assays as described below.

To test the toxicity of the particle-exposed medium from each of the respective test particles, growth media were prepared with a high concentration of each of the particles and incubated approximately 24 hrs. at 37°C with gentle rocking. For negative controls, growth medium without test particles was incubated similarly. All five aliquots of medium (with or without particulates) were centrifuged, and the supernatant of each was filtered through Millipore filter (a 0.45  $\mu\text{m}$  filter was used in the first test; a 0.22  $\mu\text{m}$  filter was used in the second test). The filtrate was then added to culture dishes containing actively growing cells. Other cultures were exposed to growth medium containing the test particles. Incubation, harvesting and counting procedures were followed as described in the *Appendix* for the ICP test. The filtrate was examined for the presence of particles. Because 200,000-400,000 particles/ml were observed in the filtrates of the first test (data not shown), a .22  $\mu\text{m}$  filter was used in the second test. Filtrates in the second test had approximately 2,000-4,000 very fine particles/ml (unfiltered diatomite suspensions used in this test contained approximately  $8 \times 10^6$  S-FC particles/ml or  $40 \times 10^6$  S-Nat particles/ml).

### **Test System: CHO-K1 Cell Line**

The Chinese hamster ovary (CHO-K1) cell line was selected for these studies for several reasons. Used in our laboratory in over 100 assays on 20 different mineral fiber samples, these cells have proven to be highly phagocytic (readily ingest or take up particles), highly proliferative (dividing once or twice per day) and sensitive to toxic particulates such as asbestos. Furthermore, the relative severity of toxic effects induced by four different refractory ceramic fibers in our in vitro CHO cell studies shows concordance with the in vivo progression of fibrosis and the incidence of lung tumors observed in long term animal inhalation studies (Hart et al., 1992a). The CHO-K1 cell line is an immortalized cell line derived from cultured hamster ovary cells (Puck, 1958). It is an anchorage-dependent (adheres to the bottom of the culture dish), epithelia-like cell type.

## RESULTS

### Cell Proliferation and Viability

Data from the ICP and CFE tests using the CHO-K1 test system (Figure 3 and 4) show a similar pattern: S-Nat is most toxic, S-FC is intermediate, and the respective toxicities of the two pure crystalline forms of silica (cristobalite and quartz) are relatively low. Figure 3 compares the ICP curves of the two DE's with the curves for UICC crocidolite asbestos (CD). (Tests for CD followed the same protocol but were not conducted simultaneously with the DE ICP tests.) Note that these comparisons are made on the basis of mass/cm<sup>2</sup> and not by number of particles/cm<sup>2</sup>. In this test system, the cell proliferation curve for cultures exposed to S-Nat is similar to the curve for cultures exposed to CD. The EC50 (concentration which reduced proliferation to 50% of negative controls) of each test particulate is provided in Table II.

The inhibition of proliferation induced by particulate suspensions contrasts sharply with the inhibition induced by the filtrate from these suspensions. When particles were removed from the medium by a .22 μm filter and then added to the cell cultures, virtually no inhibition was observed (Figure 5). However, when a .45 μm filter was used (one test), a slight depression in cell numbers was observed for both DE's (data not included). This was probably due to the quantity of fine particles observed in the filtrate.

CHO-K1 cell viability, as measured by the EAV test, was not appreciably decreased by exposure to high concentrations of the test particulates (Figure 6 and Table III). This contrasts sharply with the large differences in cell proliferation observed over the same three days of particulate exposure (Figure 7). Note that in this test, cristobalite-exposure is higher (50 μg/cm<sup>2</sup>) than that of the other four test articles (20 μg/cm<sup>2</sup>.) Cell numbers in S-

Nat- and CD-exposed cultures show almost no increase over the original number of cells plated; cristobalite, at more than twice the mass concentration of the other test particulates, is the least inhibitory and S-FC is intermediate.

### **Nuclear Abnormality Assay**

The results from the nuclear abnormality assay (Figure 8) agree with the results from the ICP and CFE assays; the highest incidence of nuclear abnormalities was observed in the S-Nat cultures, the incidence with S-FC was second highest, and the two crystalline reference particulates had relatively low incidences.

The types of visible cell damage induced by each of these four particulates can be seen in the photomicrographs of acridine orange-stained cells (Figures 9-14). The photographs are in pairs: the first was taken with fluorescence microscopy, and the second depicts the same field with phase contrast optical microscopy (PCOM). In the fluorescent photographs, the cytoplasm of the cells is orange and the nuclei are yellow. In the PCOM photographs, the cells appear as opalescent bodies in tones of blue, yellow and green.

Unexposed CHO-K1 cells, growing in culture medium without any test particulates, are seen in Figure 9A and B. Note the micronucleus (arrow). In unexposed CHO-K1 cells the background incidence of nuclear abnormalities ranges from 2-7%. One or two small, distinct micronuclei per cell is typical of genotoxic chemical exposure; however, as can be seen in the fluorescent photomicrographs, nuclear abnormalities induced by particulates is typically far more diverse, including multiple and grossly distorted nuclei as well as micronuclei.

Shapes, sizes and locations of the test particles can be seen in the PCOM photographs of the exposed cultures, even though fixing and staining procedures wash away a portion of the particles. The many fibrous shapes as well as non-fibrous particles of both diatomite dusts are visible in Figures 10B, 10D, 10F and 11B. This is in contrast to the two crystalline silica reference particulates, in which only non-fibrous particles can be seen (Figures 12B and 13B). The two DE's are also similar in that each has a population of large particles as well as fine particles, however S-Nat clearly has more of the latter. Likewise, the range of sizes present in the two crystalline reference particulates appears similar but the distribution does not: quartz has many more small particles than does cristobalite. Finally, note that the cells have accumulated large numbers of particles, most of which appear to be within the cells.

A review of the fluorescent photographs of exposed cultures gives the impression of a range of gross cytoplasmic and nuclear abnormalities. Cells with multiple and irregularly shaped nuclei are seen. Visible cellular abnormalities appear less severe in the cristobalite- and quartz-exposed cultures. In the S-Nat-exposed cultures, many nuclei appear to have little or no cytoplasm (orange-fluorescing) remaining around them (Fig 10C, E). Note the orange-fluorescing particles in these photographs. With PCOM (Figure 10D, F) these same particles appear to be a non-fibrous subpopulation of the diatomite. The same pattern of fluorescence was observed in S-Nat that was incubated in medium without cells and stained with acridine orange; therefore it was concluded that this phenomenon was not a result of cellular interactions with the particles. In contrast to the S-Nat photographs, those of S-FC (Figure 9) do not have any of these orange-fluorescing particles.

As with the ICP data, the INA curves for S-Nat and S-FC are comparable to the INA curve for UICC crocidolite asbestos (when concentrations are calculated as mass/unit surface area). Qualitative differences as well as similarities can be observed by comparing cells

exposed to the CD fibers (Figure 14) with cells exposed to diatomite particles. Acridine orange stained CD-exposed cells give a general impression of nuclear disruptions with little effect on the cytoplasm. Multiple nuclei, including one or more micronuclei are common, and to a lesser extent, enlarged cells with multi-lobed-appearing nuclei are observed. On the other hand, cells exposed to the diatomites (Figures 15 and 16, 1000 X) appear to have morphological distortions and both nuclear and cytoplasmic membranes are indistinct. These abnormalities are not observed in the photographs of cells exposed to each of the two reference particulates, Cristobalite and  $\alpha$ -Quartz.

## DISCUSSION

At this time, no known in vitro test systems can be used to predict the whole-organism effects of inhaled particles. Thus, the findings of this study should not be misconstrued to be, in any way, indicative of what possible effects the test particulates could have on an organism following inhalation exposure. However, the in vitro toxicity of diatomites to cultured CHO-K1 cells was sufficiently clear to indicate that further testing is needed to determine the potential toxicity of DE.

Assays measuring cell proliferation, colony forming efficiency, and the induction of nuclear abnormalities, showed striking, concentration-related toxicity of DE to cultured CHO-K1 cells. Cell viability, on the other hand, was only slightly decreased by diatomite exposure. Toxicity from soluble chemicals was ruled out when no effects were observed in cells exposed to filtered DE-leachate. These observations suggest that the mechanism of toxicity is primarily a disruption of cell division resulting from the cellular uptake (phagocytosis) of particles. CHO-K1 cells divide rapidly and, according to our observations, readily take up a variety of different types of particles by phagocytosis, two features which make them sensitive to this type of toxic mechanism.

The several particulates evaluated in the present study were not equally toxic. In an attempt to determine the causes of these differences in toxicity, various parameters (crystallinity, surface area, particles/ $\mu\text{g}$ , dimensions, % fibrous particles) of the four dusts were compared (Tables I and II). Crystallinity was not directly related to toxicity; S-Nat was the most toxic of the silica dusts, but it is primarily amorphous. Nor was particle number directly related to toxicity; the number of particles/ $\mu\text{g}$  was similar in S-Nat and quartz, yet the former was considerably more toxic than the latter. One possible cause of toxic differences could be a combination of surface area and surface chemistry resulting in

different adsorbencies of the various particulates for cellular constituents. S-Nat was more toxic than FC, and S-Nat is estimated to have a 10-fold greater surface area than FC.

Another possible cause of toxic differences could be percentage of particles that are fibrous (length/diameter  $\geq 3$ ). When EC50's are calculated as number of fibers longer than 7.5  $\mu\text{m}$  per  $\text{cm}^2$ , the EC50's for Nat, FC, cristobalite and CD are very similar to each other (214, 259, 214 and 384, respectively,  $\times 10^3$ ). Quartz and  $\text{TiO}_2$  had no fibrous particles. Further investigations of DE materials are needed to test these hypotheses. A clarification of the relationships between toxicity and particle characteristic could provide a major step toward an understanding of the cellular mechanisms of particulate toxicology.

Further in vitro testing is advised, utilizing cultured cells derived from lung tissues, such as normal rat alveolar macrophages, rat or human airway epithelium and/or lung mesothelium. Lung macrophages are a key cell in the pathogenesis of respirable particles in the whole organism, particularly in lung clearance. These highly phagocytic and mobile cells ingest particles in the lung, subject them to digestive and corrosive secretions, and attempt to carry the particles up and out of the respiratory tract. Particles that chemically or physically interfere with these clearance functions may be more pathogenic to the organism than particles which the macrophages are able to either degrade or carry out of the lungs. Lung mesothelial cells may be a target tissue of inhalation toxicants in that pulmonary mesothelioma has been associated with whole-animal exposure to some mineral fibers. (Hesterberg et al., 1991). Airway epithelium may provide a protective barrier to some particulates and may therefore be less sensitive than other tissues to the toxic effects of some particulates. All of these lung cell types are available for testing in the MTC In Vitro Laboratory, including both human and rodent cell lines as well as normal rodent and human primary cells.

Other DE test particulates should also be evaluated, to measure the impact of surface area, surface chemistry and particle size, shape and number of particles/unit culture surface area. In vitro testing of different size-separated fractions of the several diatomaceous earth products as well as size-selected reference chemical particulates could help clarify the source(s) of the observed toxic effects.

## REFERENCES

- Clark, G. 1981. Staining Procedures, Fourth Edition. Waverly Press, Inc.
- Hart, G.A., Newman, M.M., Bunn, W.B. and Hesterberg, T.W. Cytotoxicity of refractory ceramic fibers to chinese hamster ovary cells in culture. 1992a. Toxicology In Vitro 6(4):317-362.
- Hart, G.A., M.M. Newman, W.B. Bunn, and T.W. Hesterberg Importance of fiber dimensions in the cytotoxicity of mineral fibers to chinese hamster ovary cells in culture. The Toxicologist, March, 1992b.
- Hesterberg, T.W., and Barrett, J.C. 1985. Induction by asbestos fibers of anaphase abnormalities: mechanism for aneuploidy induction and possibly carcinogenesis. Carcinogenesis 6:473-475.
- Hesterberg, T.W., R. Mast, E.E. McConnell, O. Vogel, J. Chevalier, D.M. Bernstein and R. Anderson. Chronic inhalation toxicity and oncogenicity study of refractory ceramic fibers in Fisher 344 rats. The Toxicologist 11:85(254), 1991.
- Hesterberg, T.W., Vu, V., McConnell, E.E., Chase, G.R., Bunn, W. B. and Anderson, R.. Use of Animal Models to Study Man-made Fiber Carcinogenesis. In "Cellular and Molecular Aspects of Fiber Carcinogenesis", Current Communications in Cell and Molecular Biology, (eds. C. Harris, J. Lechner, and B. Brinkley), Cold Spring Harbor Laboratory Press, pp. 183-205, 1991.
- Puck, T.T. J. Exp. Med. 108:945, 1958.
- Sincock, A. M., Delhanty, J. D. A., and Casey, G. 1982. A comparison of the cytogenetic response to asbestos and glass fibre in Chinese hamster and human cell lines. Demonstration of growth inhibition in primary human fibroblasts. Mutat. Res. 101, 257-268.

## ACKNOWLEDGEMENTS

The data in this report was compiled through the cooperation of the following Mountain Technical Center Laboratories. Individuals who were particularly instrumental in the technical work are mentioned:

**MTC Particle Preparation Laboratory, W. Miiller**

Size separation of diatomite test particles: Barry Fitzpatrick.

**MTC Microstructural Analysis Laboratory, R. Hamilton**

SEM dimensional analysis and photography of diatomite test particles: Frank D'Ovidio, John Strothers and Cathy Smith.

**MTC In Vitro Laboratory, G.A. Hart**

PCOM and Fluorescent microphotographs: Lisa Kathman.

Technical Support for in vitro testing: Lisa Kathman and Mildred Newman .

**Study Director:** T.W. Hesterberg, Ph.D.

**Study Supervisor:** G.A. Hart, M.A.

Figure 1. SEM microphotographs of diatomite test chamber. (A and B) magnified X 1000 & 2500, respectively. C-D.: s-FC DE, magnified X 1000 & 2500, respectively.

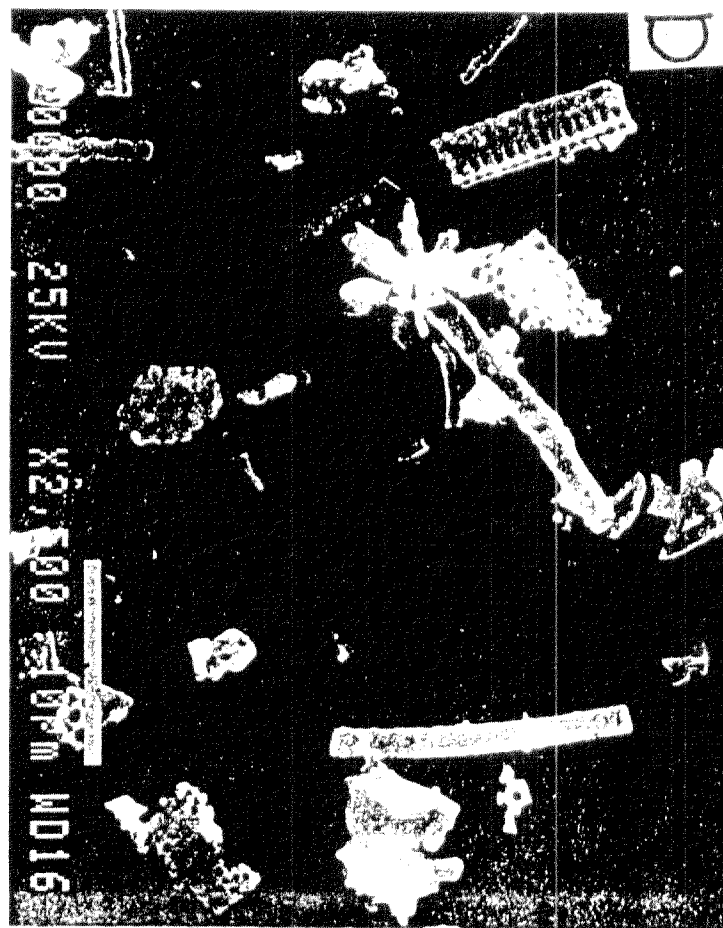
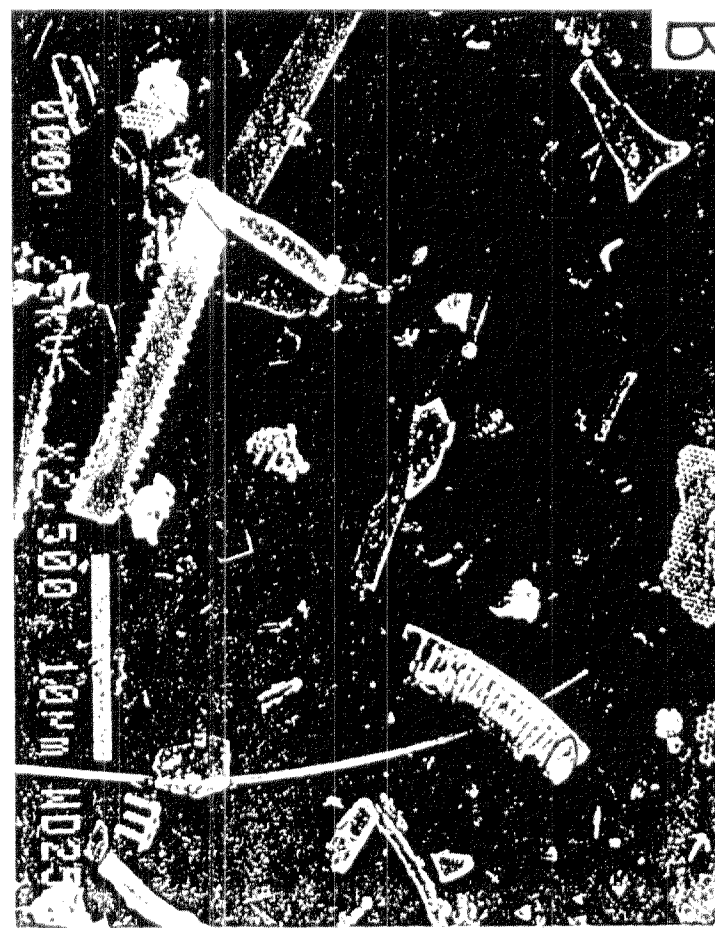
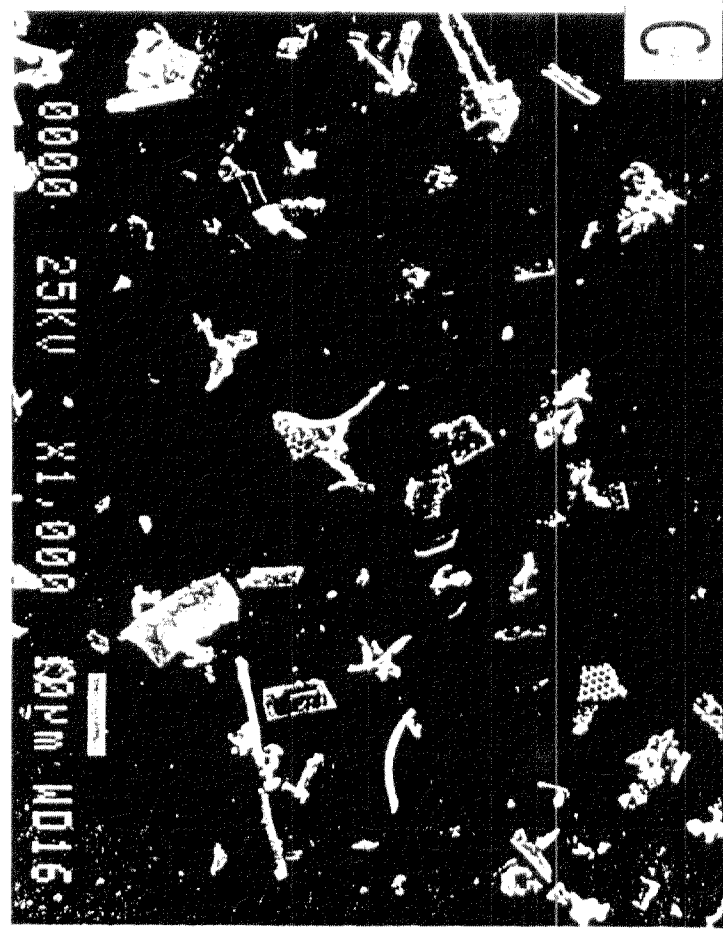
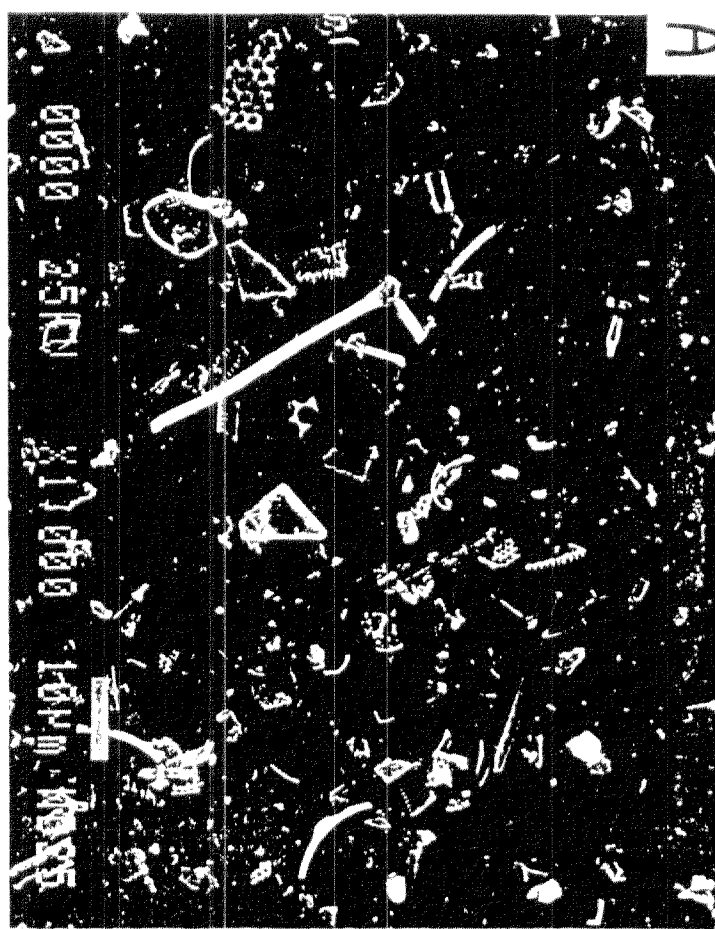


Figure 1. SEM Microphotographs of Crystalline Silica References: Cristobalite, E.-F.; Cristobalite, magnified X 1000 & 2500, respectively. G.-H.: alpha-Quartz, magnified X 2000 & 5000, respectively.

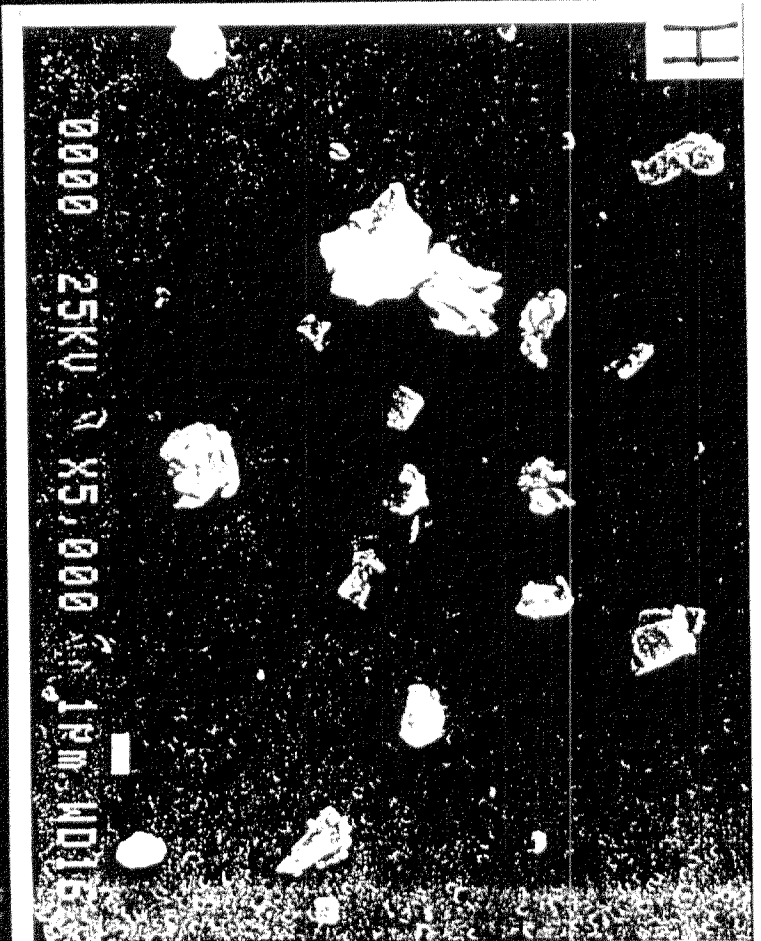
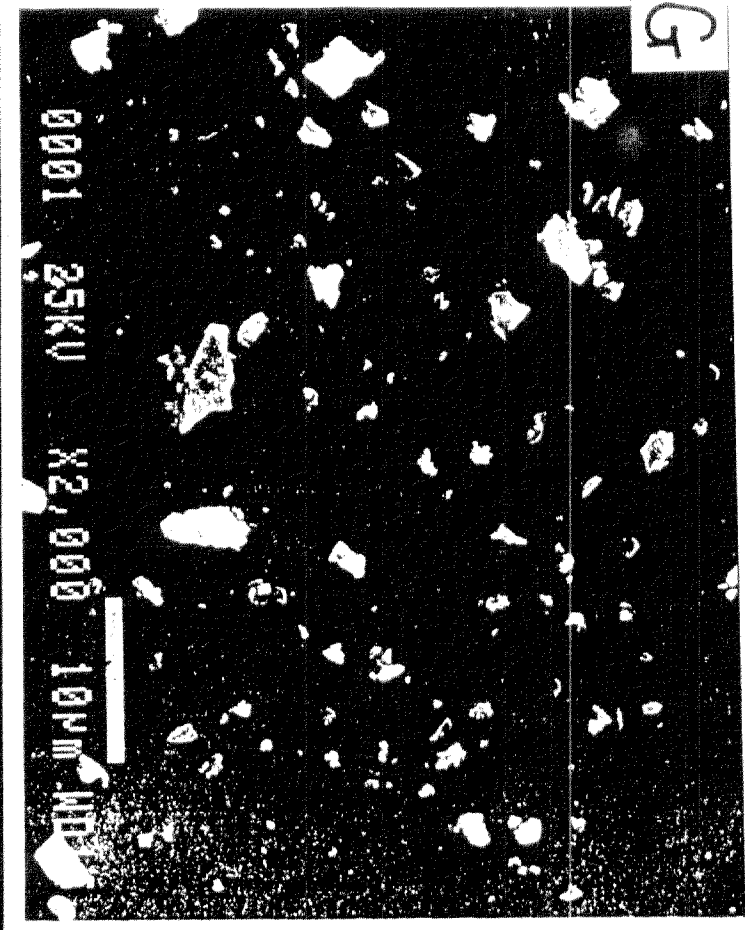
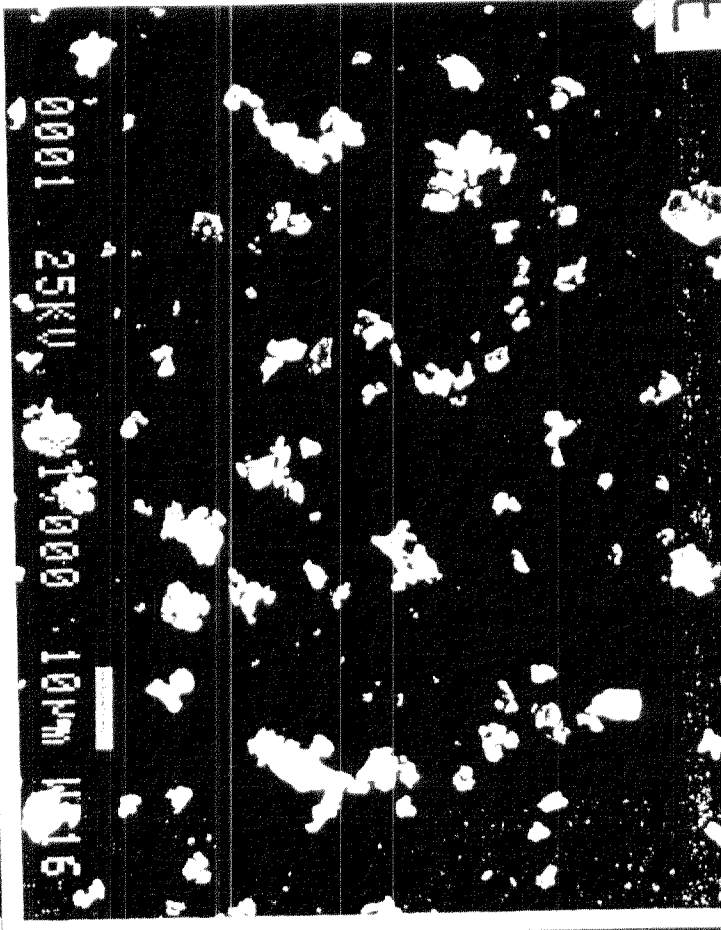
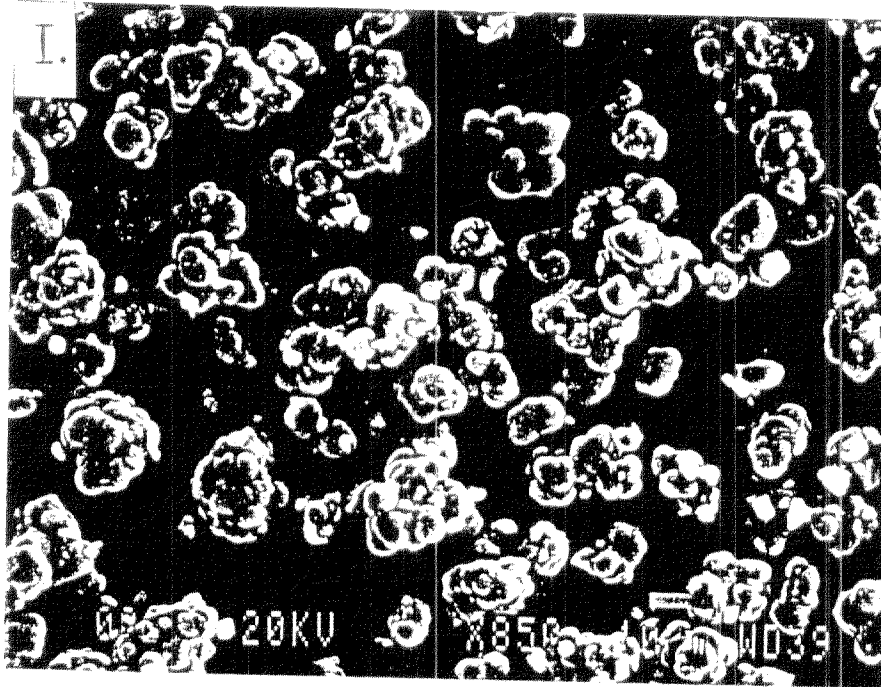


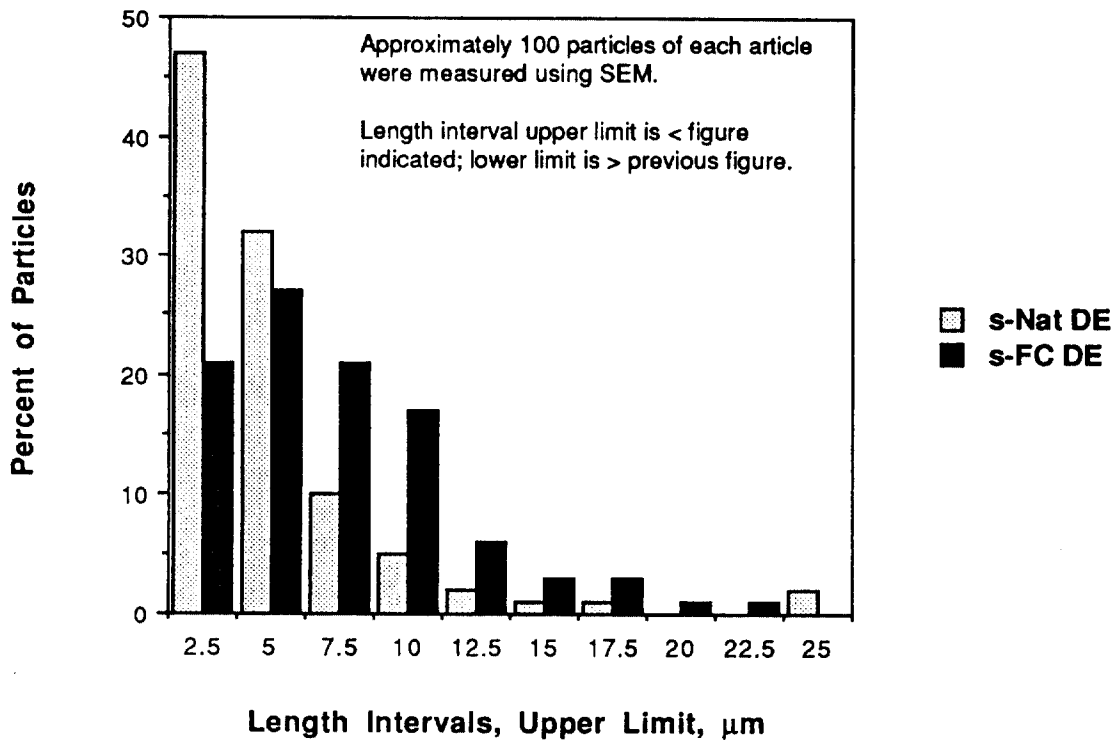
Fig 1. I. Titanium Dioxide  
magnification estimated at approximately 1000.



*Titanium Dioxide*

77

**Fig. 2. Comparison of Particle Lengths**



23

**Fig. 3a. Inhibition of Proliferation (CHO K1 Cells)**

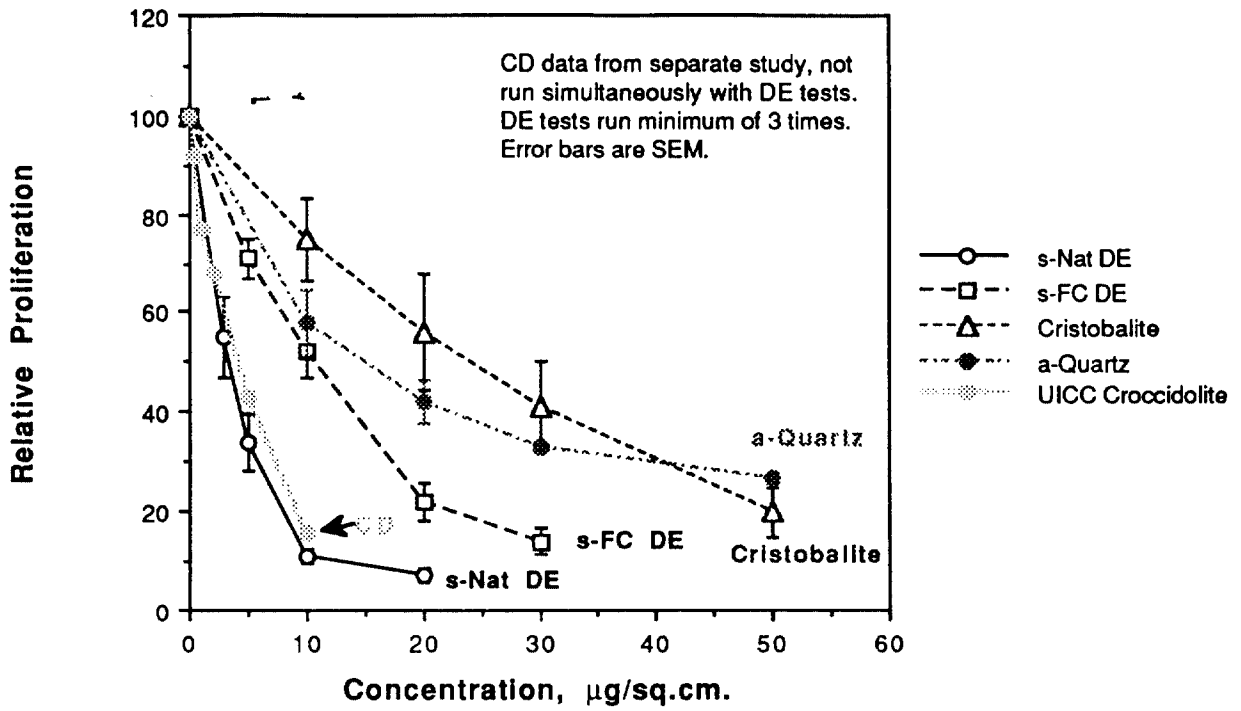
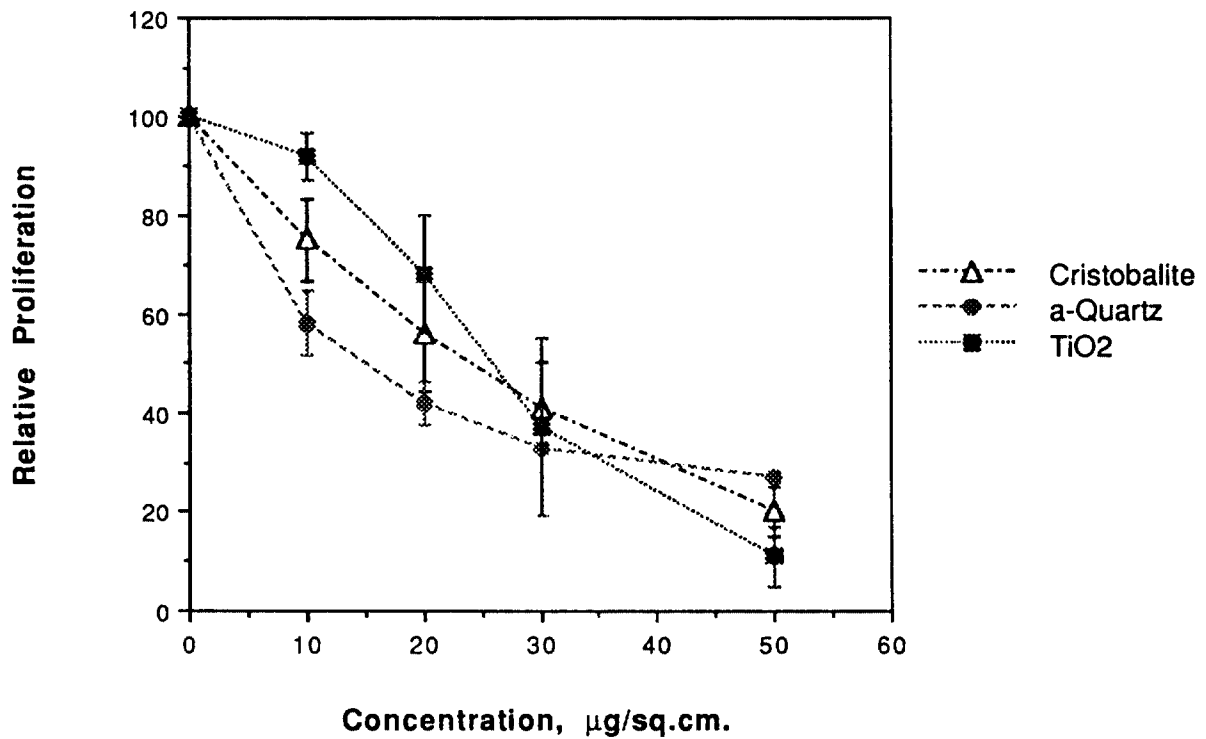


**Fig. 3 b. Inhibition of Proliferation Cristobalite, a-Quartz and Titanium Dioxide**



24

**Fig. 4. Colony Forming Efficiency  
(CHO K1 Cells)**

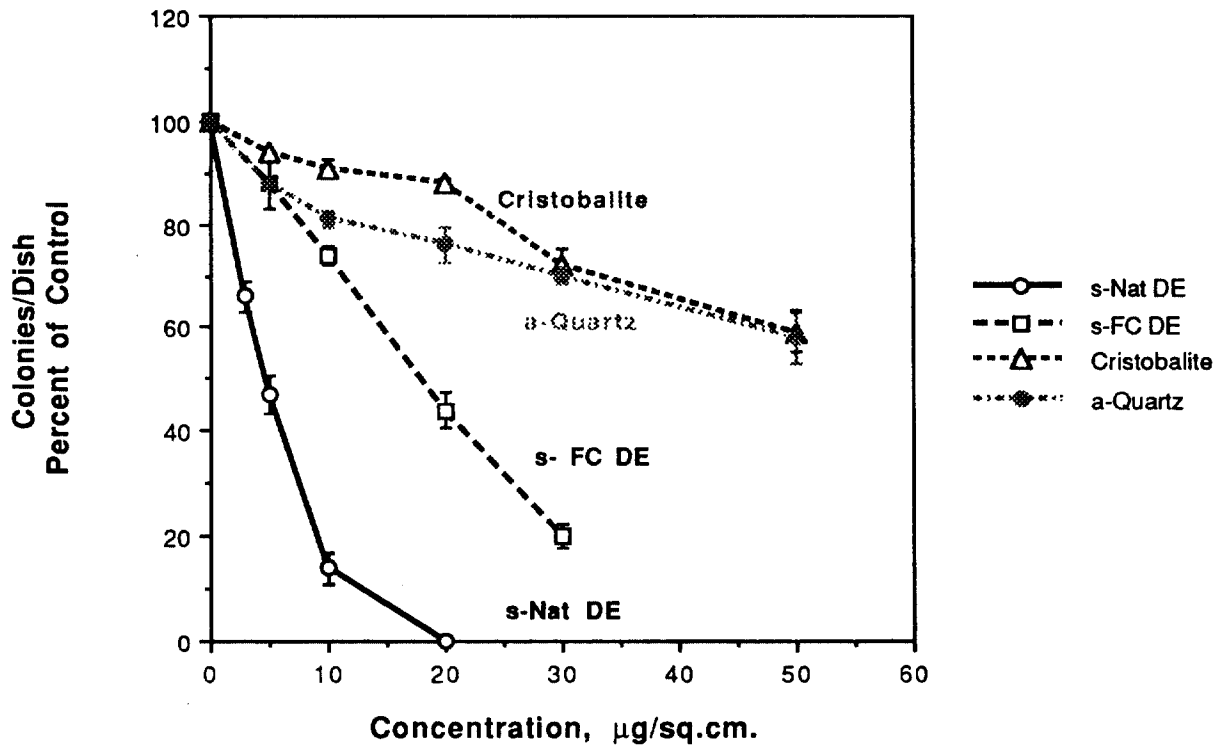
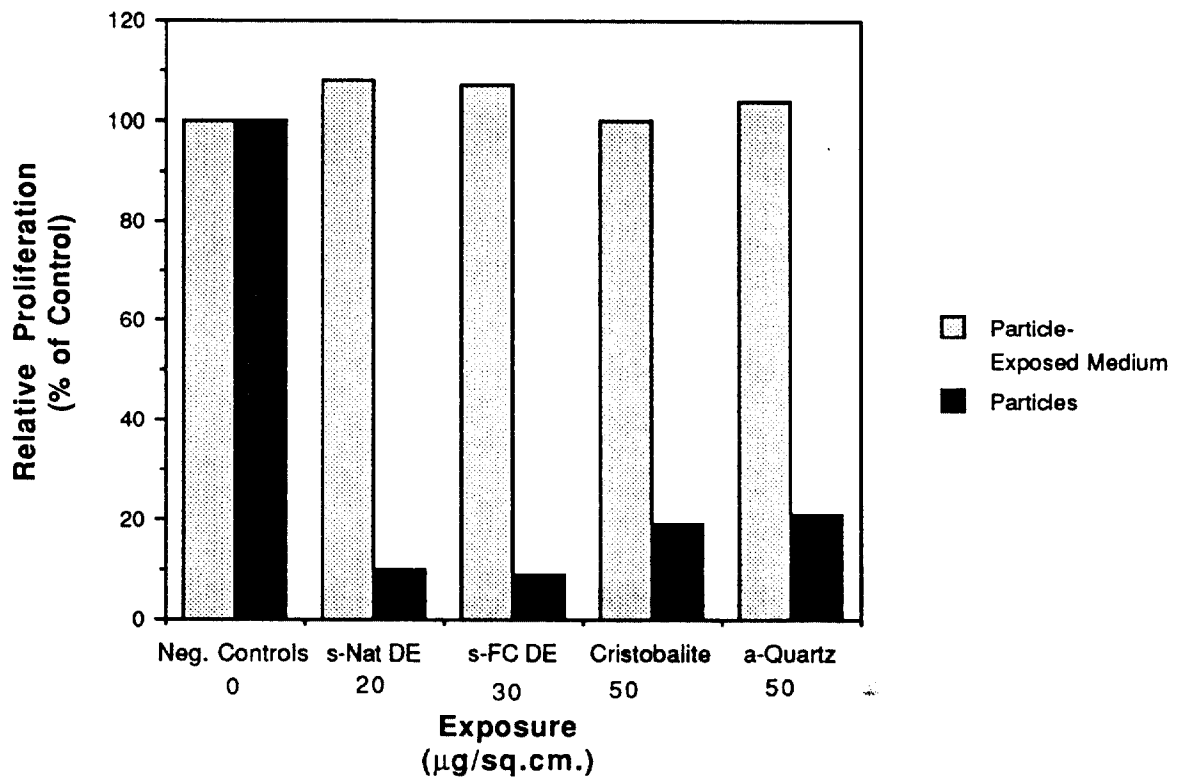


**Fig. 5. Inhibition of Cell Proliferation with Particulates v. Particle-Exposed Medium**



26

### Fig. 6. Cell Viability

After 1, 2 and 3 Days of Particle Exposure.

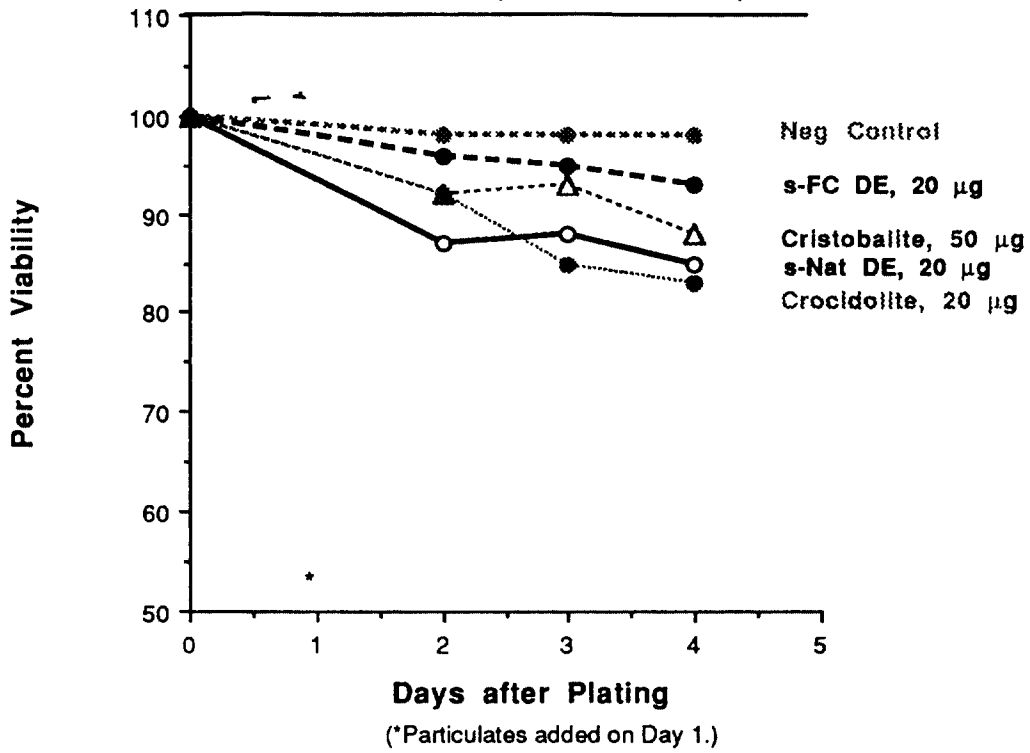
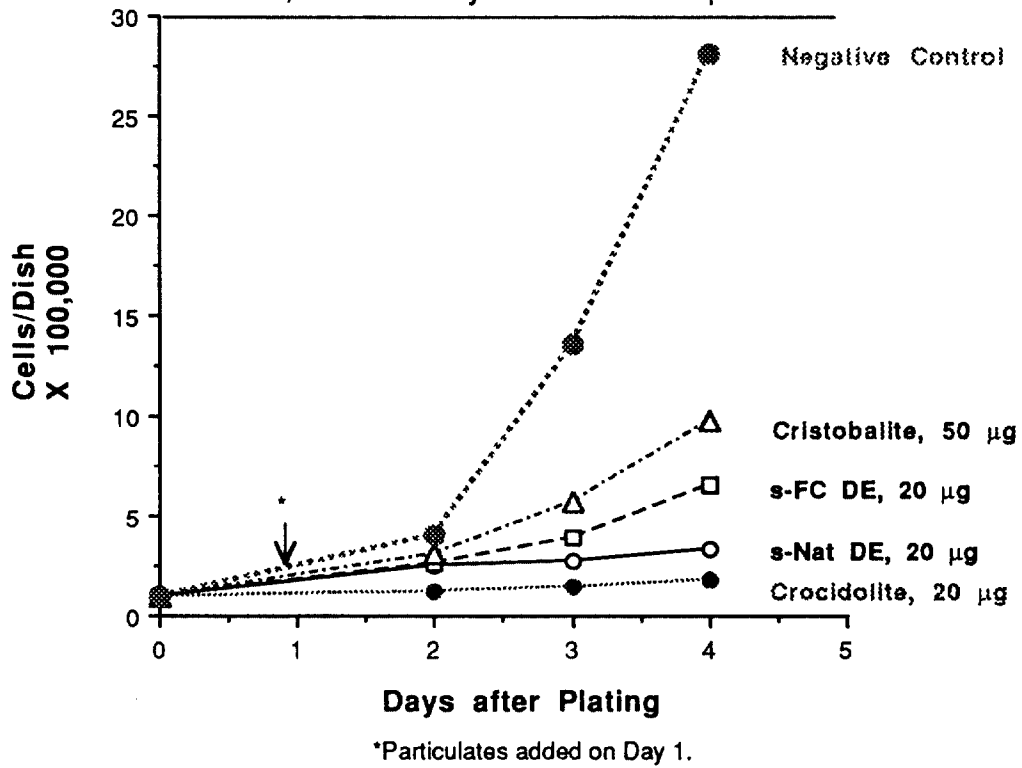


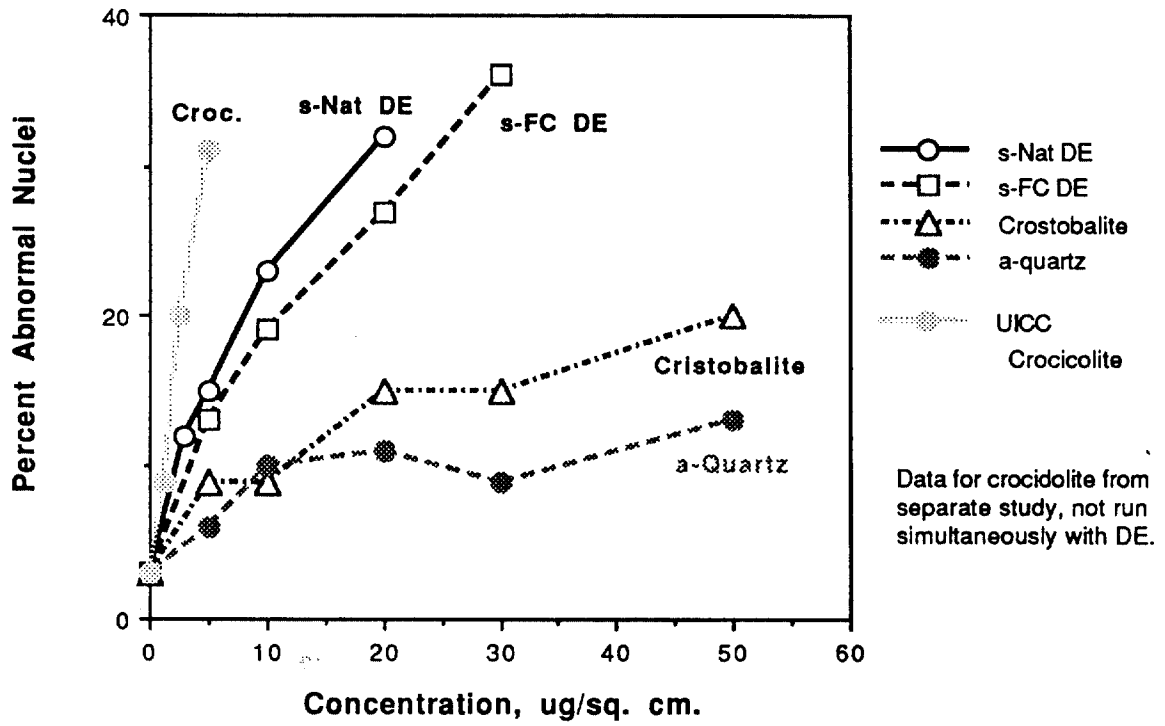
### Fig. 7. Cell Proliferation

After 1, 2 and 3 Days of Particle Exposure.



27

**Fig. 8. Induction of Nuclear Abnormalities (CHO Cells)**



Handwritten signature or initials.

Fig. 9. Normal, unexposed CHO-K1 cells growing in culture. A.: Fluorescent light. B: PCOM. White arrow indicates micronucleus.

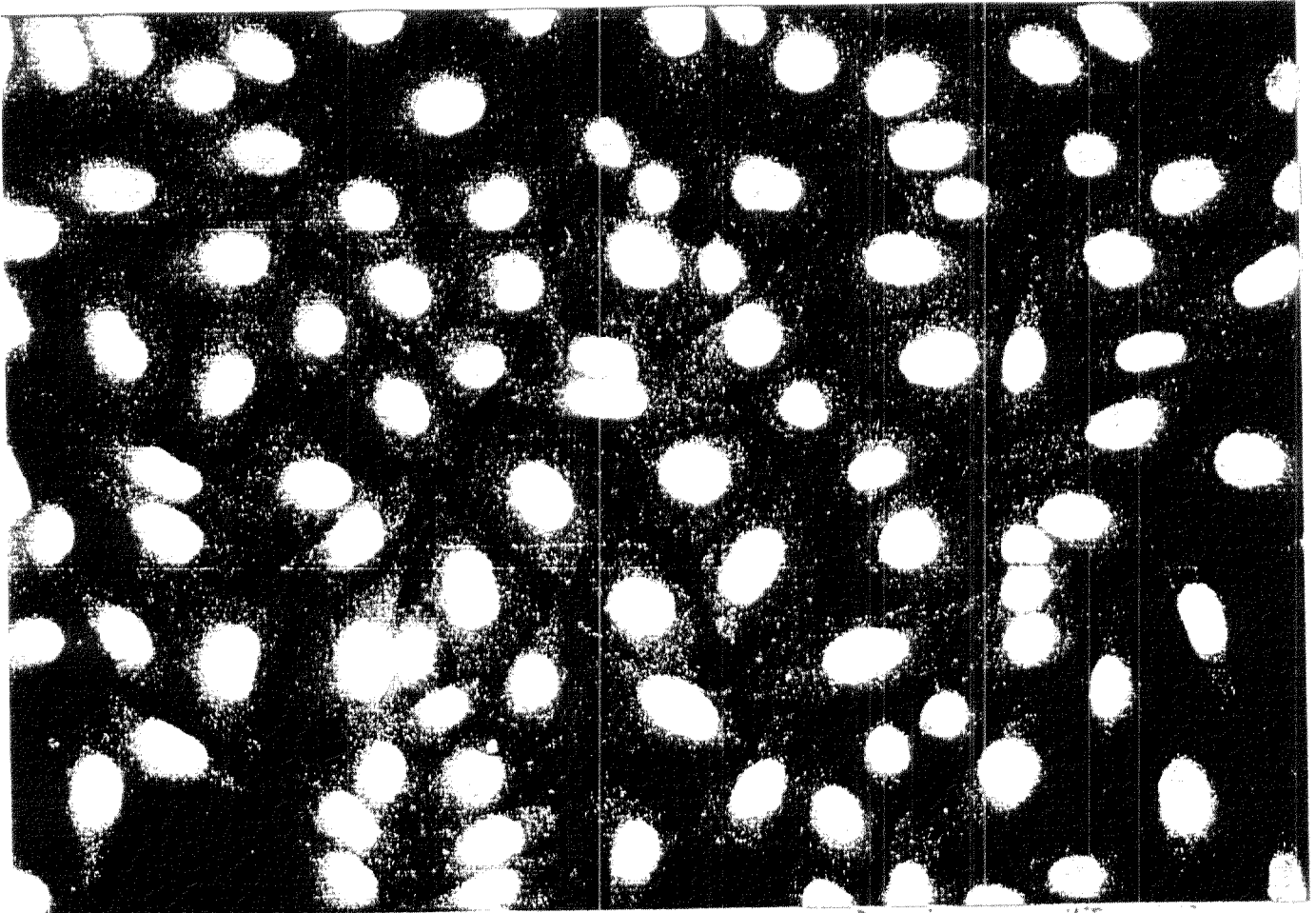
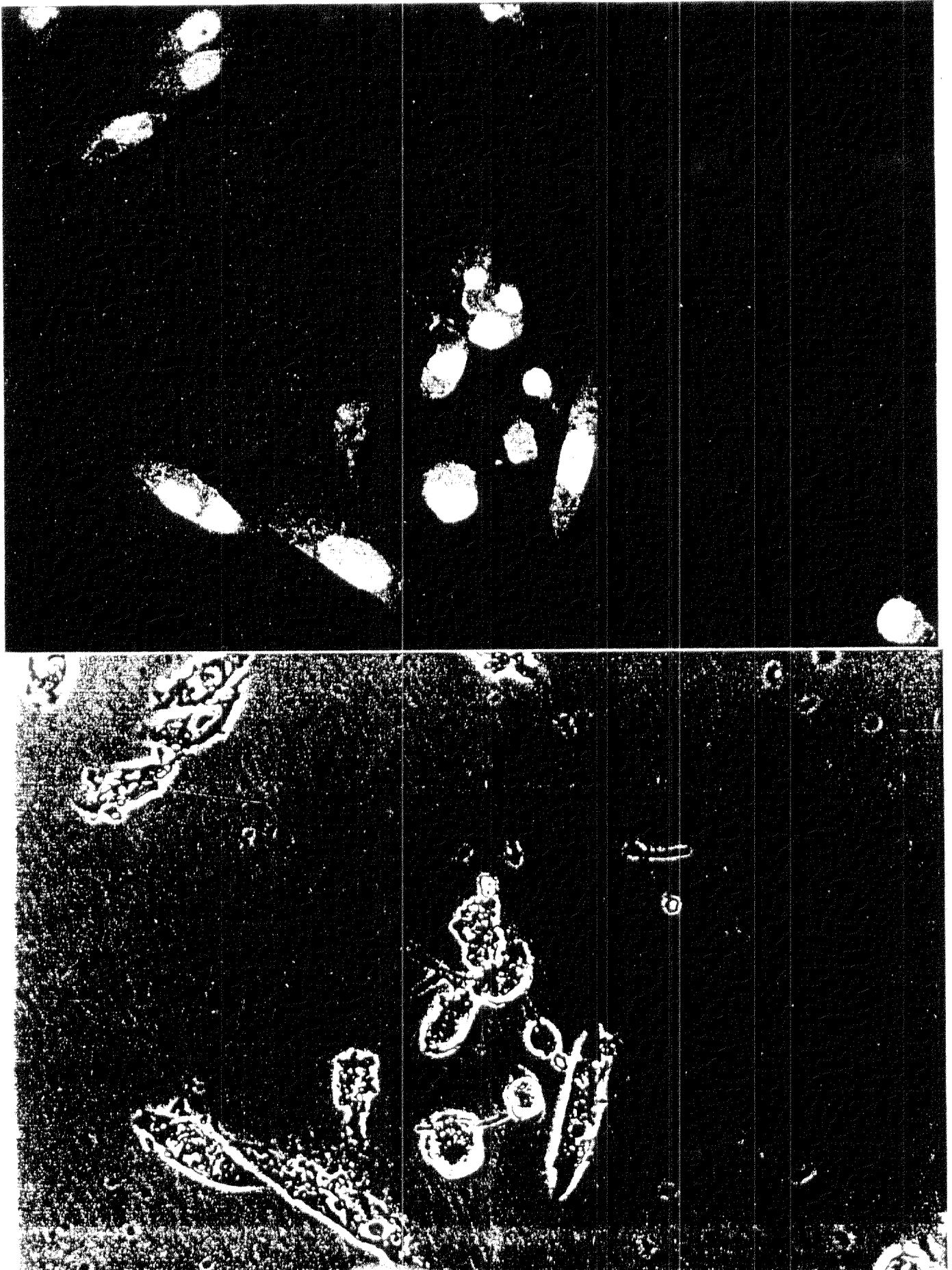


Fig. 10A-B. CHO-K1 cells exposed to s-Nat DE, 10  $\mu\text{g}/\text{sq. cm}$ . A.: Fluorescent light.  
B: PCOM. X400.



30

Fig. 10. C-D. CHO-K1 cells exposed to s-Nat DE, 20  $\mu\text{g}/\text{sq. cm}$ . C.: Fluorescent light. Note orange particles separate from gold nuclear material. D: PCOM. Note cells are associated with numerous particles which appear to be in and/or on the cells. X400.

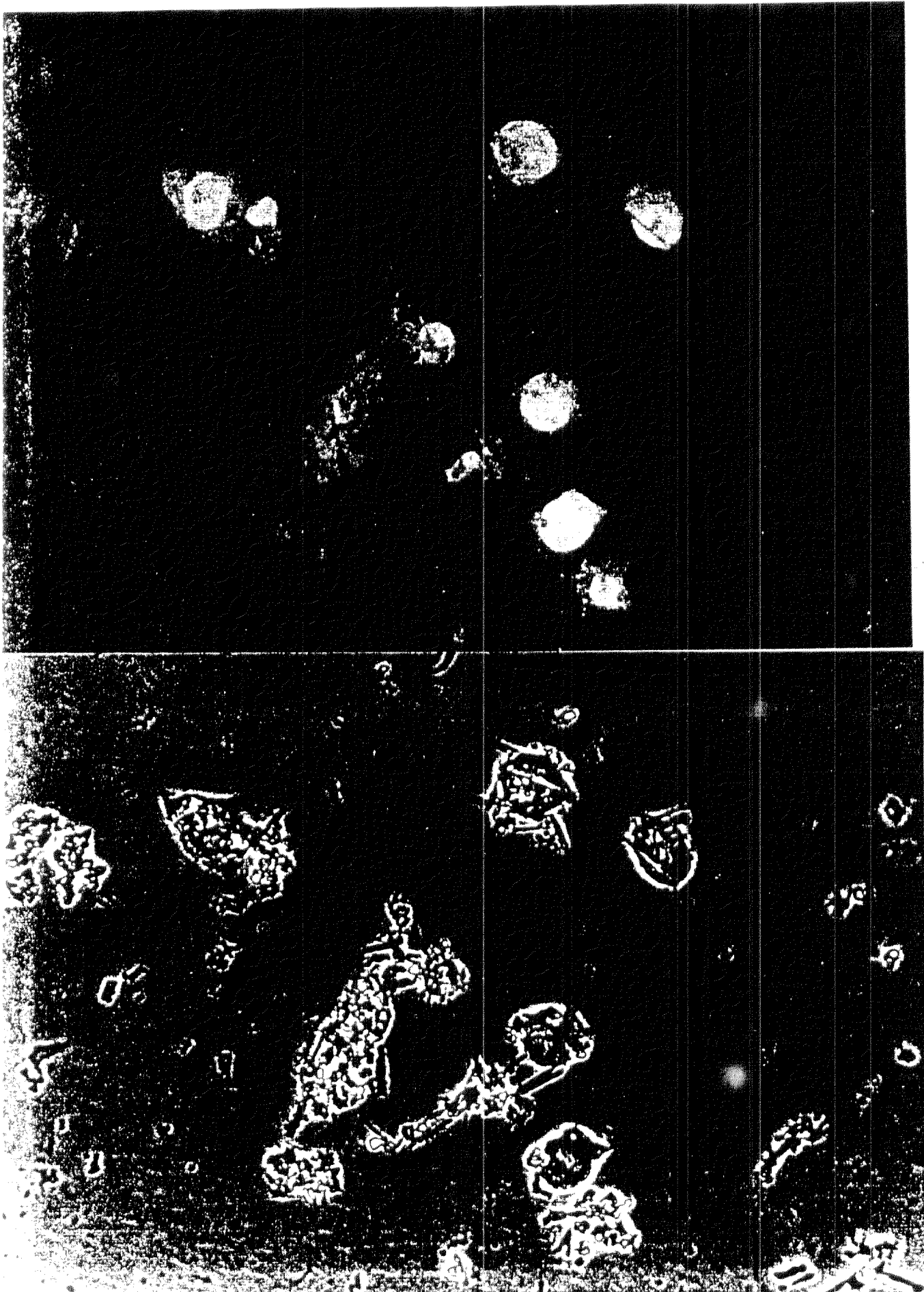
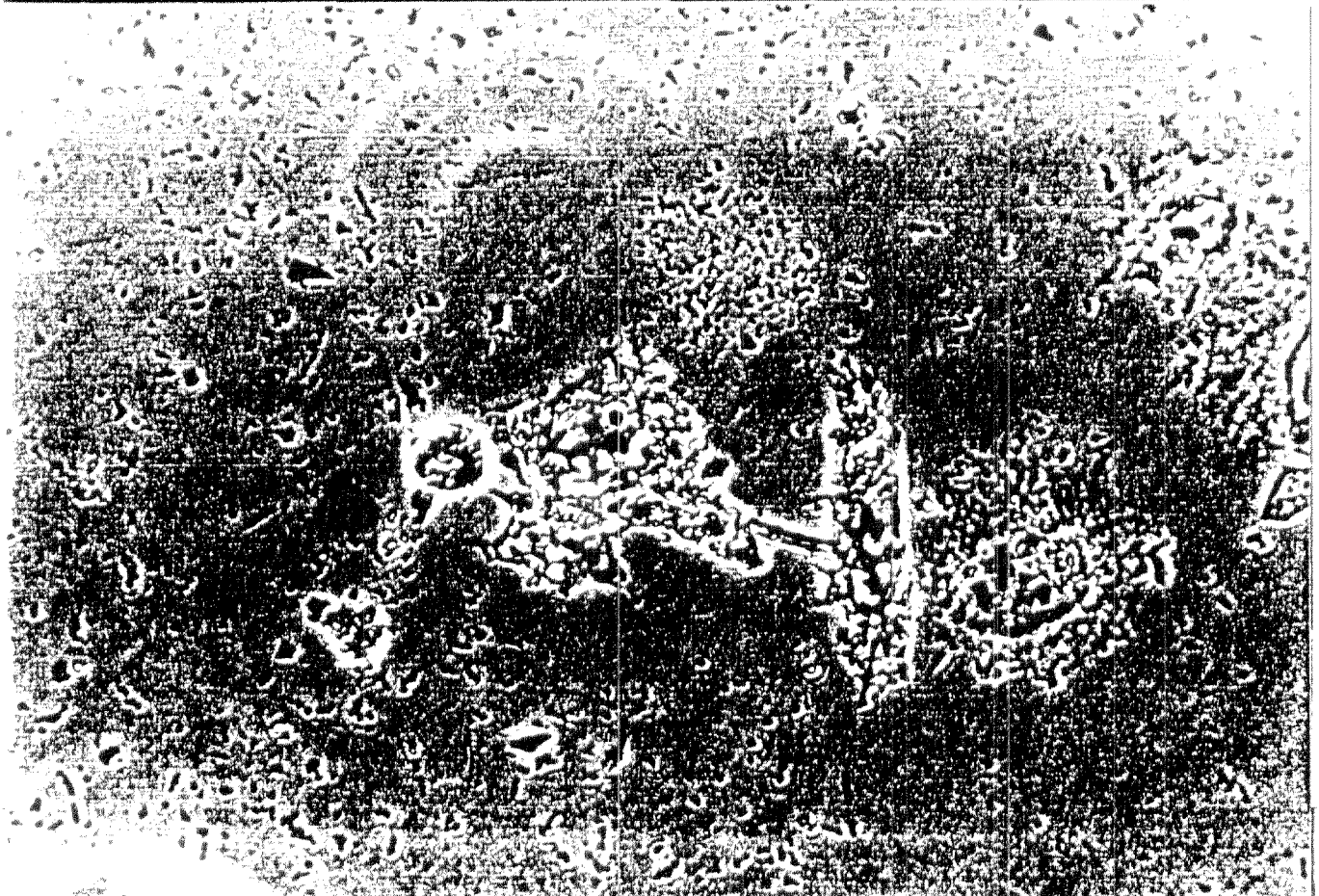
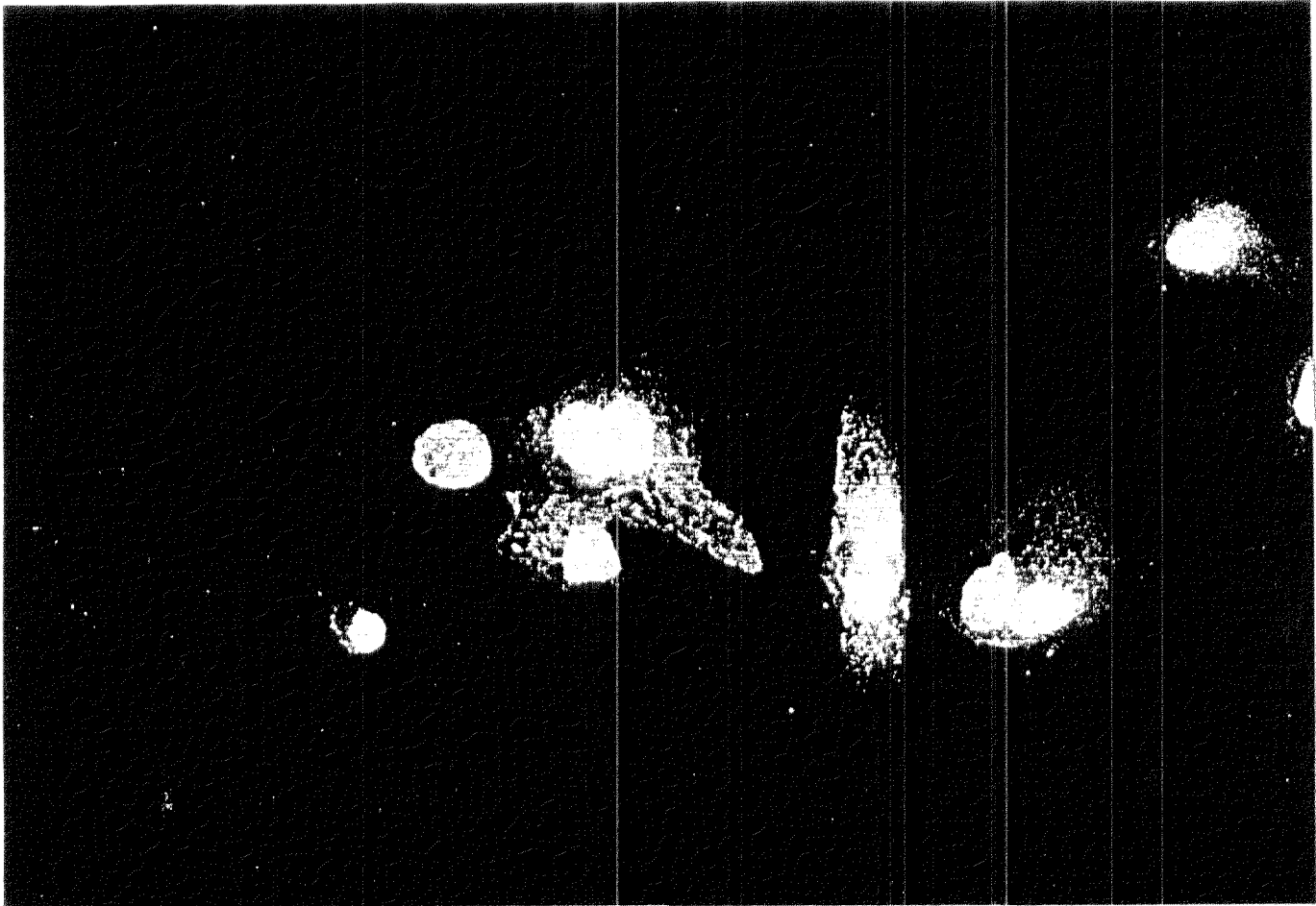
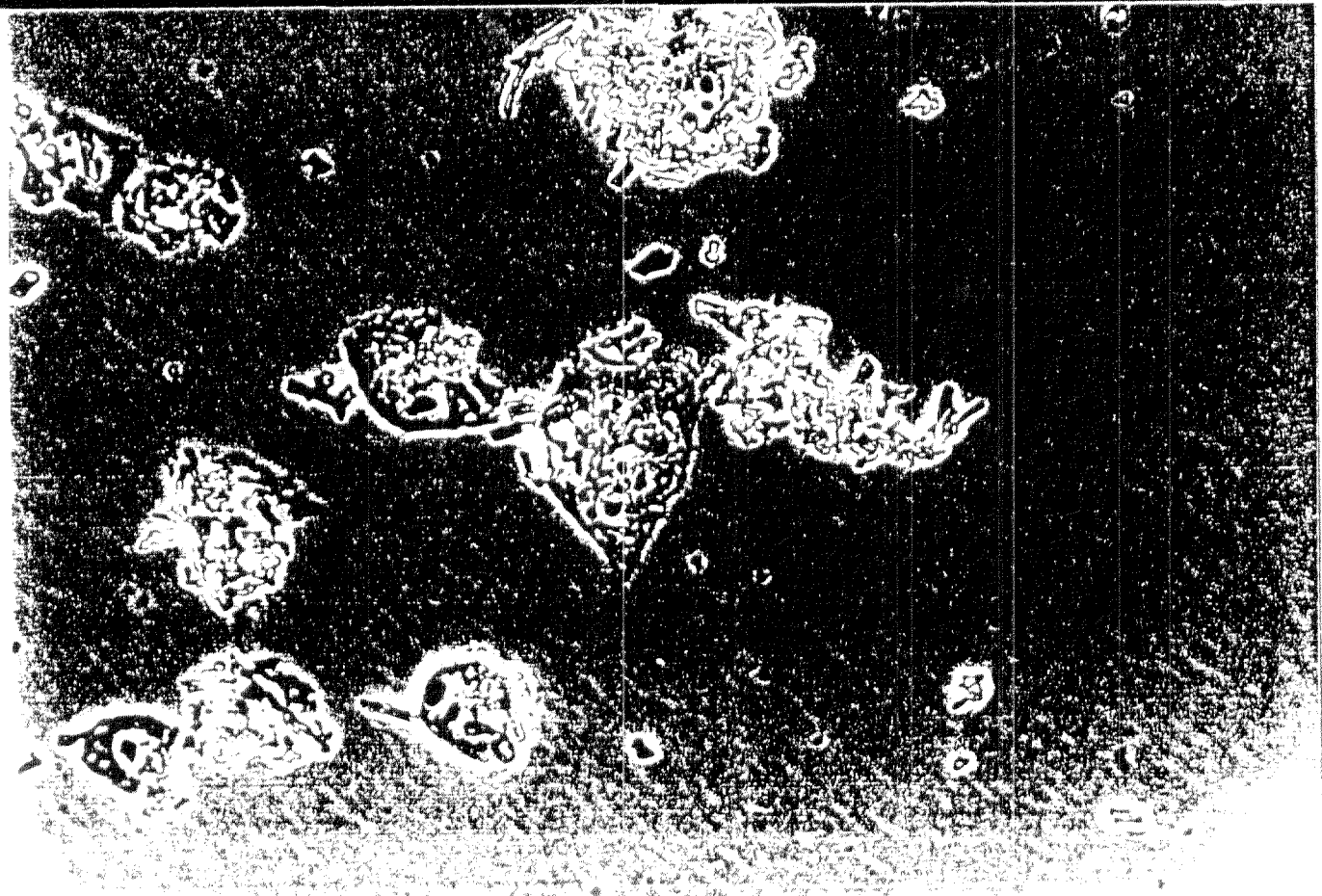
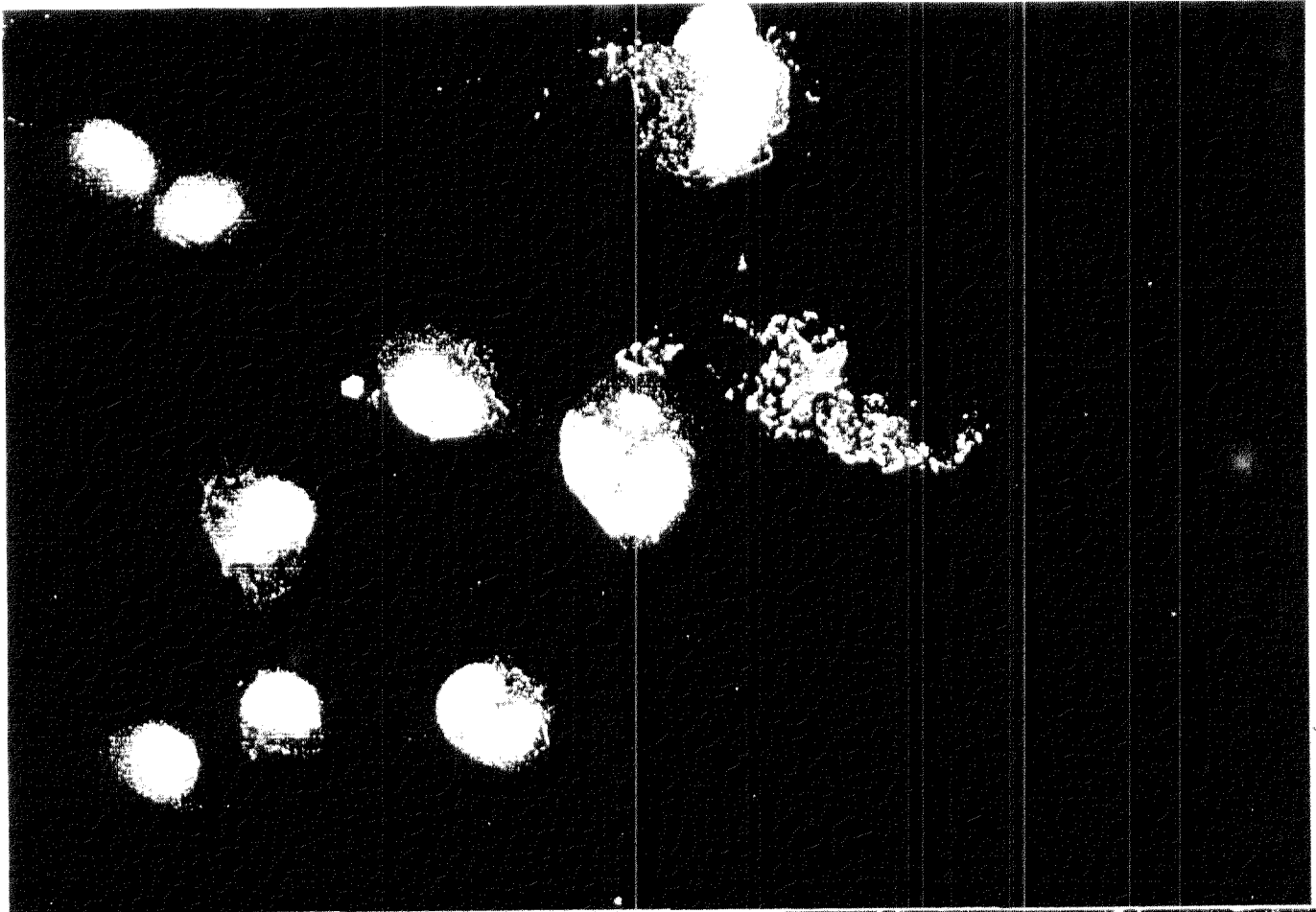


Fig. 10. E-F. CHO-K1 cells exposed to s-Nat DE, 20  $\mu\text{g}/\text{sq. cm}$ . E.: Fluorescent light.. Note cytoplasm flouresces yellow rather than orange. F: PCOM. X400.



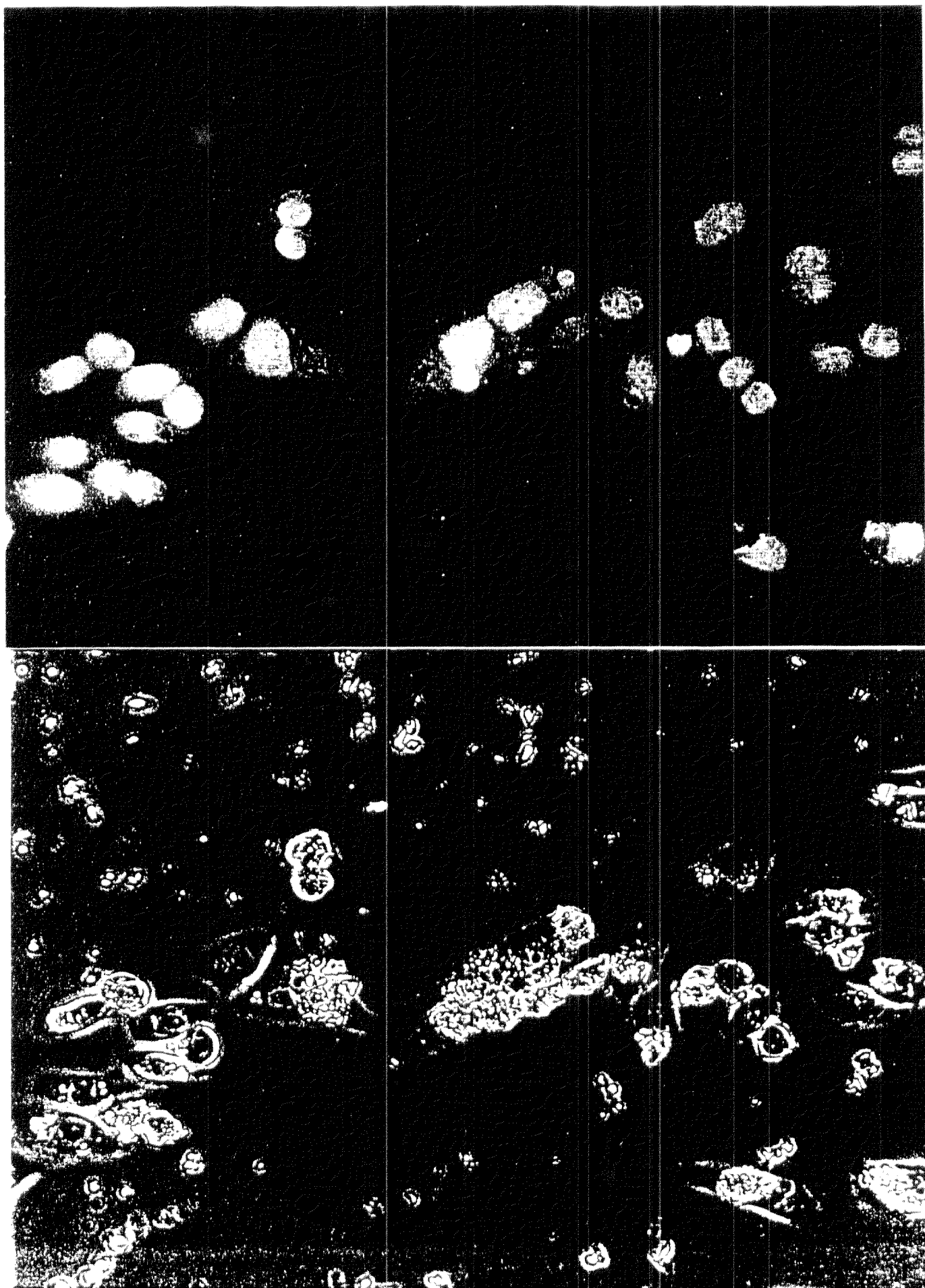
37

Fig. 11. A-B. CHO-K1 cells exposed to s-FC DE, 30  $\mu\text{g}/\text{sq. cm}$ . A.: Fluorescent light.  
B: PCOM. X400.



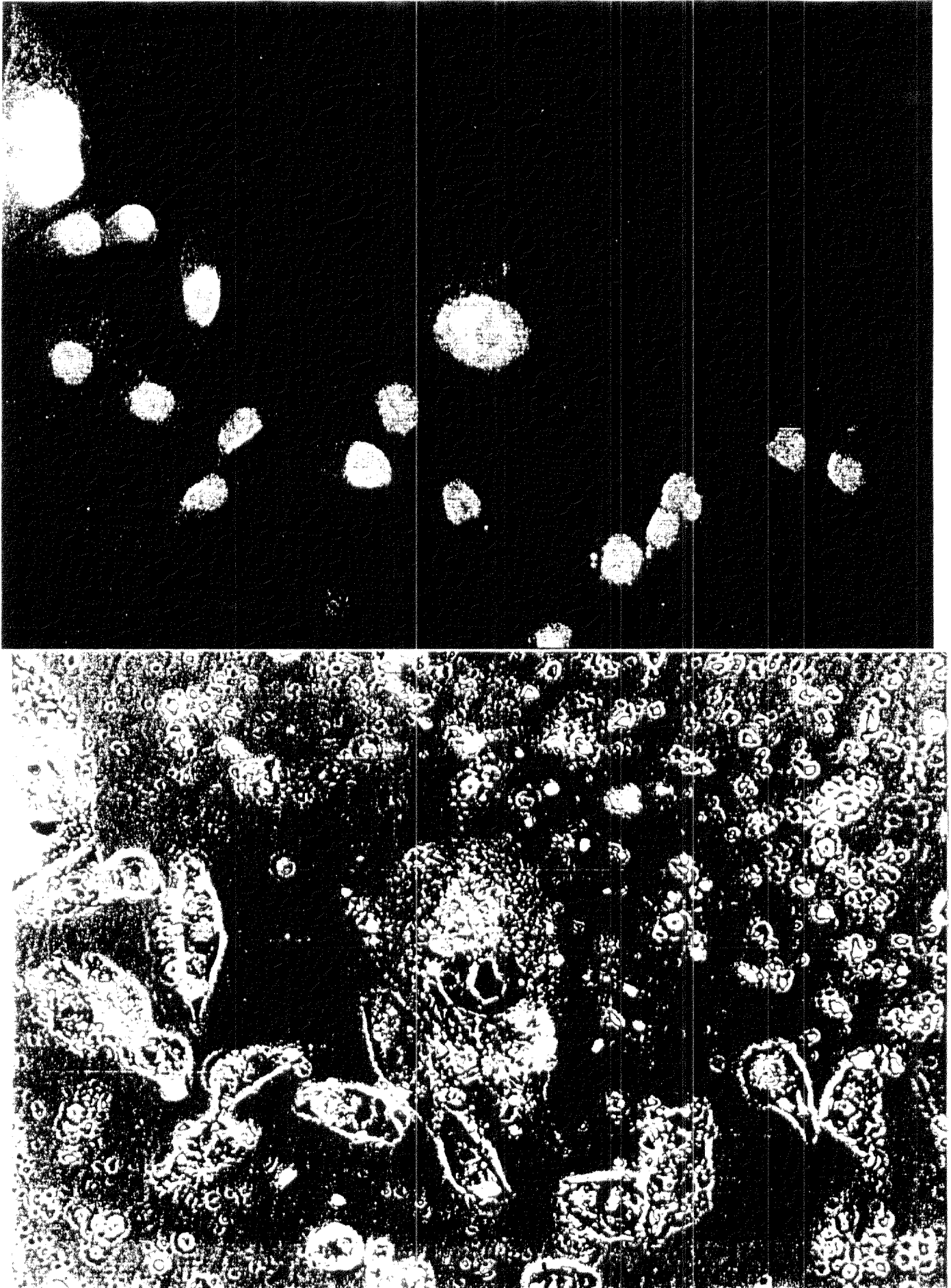
33

Fig. 12. A-B. CHO-K1 cells exposed to cristobalite, 30  $\mu\text{g}/\text{sq. cm}$ . A.: Fluorescent light. B: PCOM. X400.



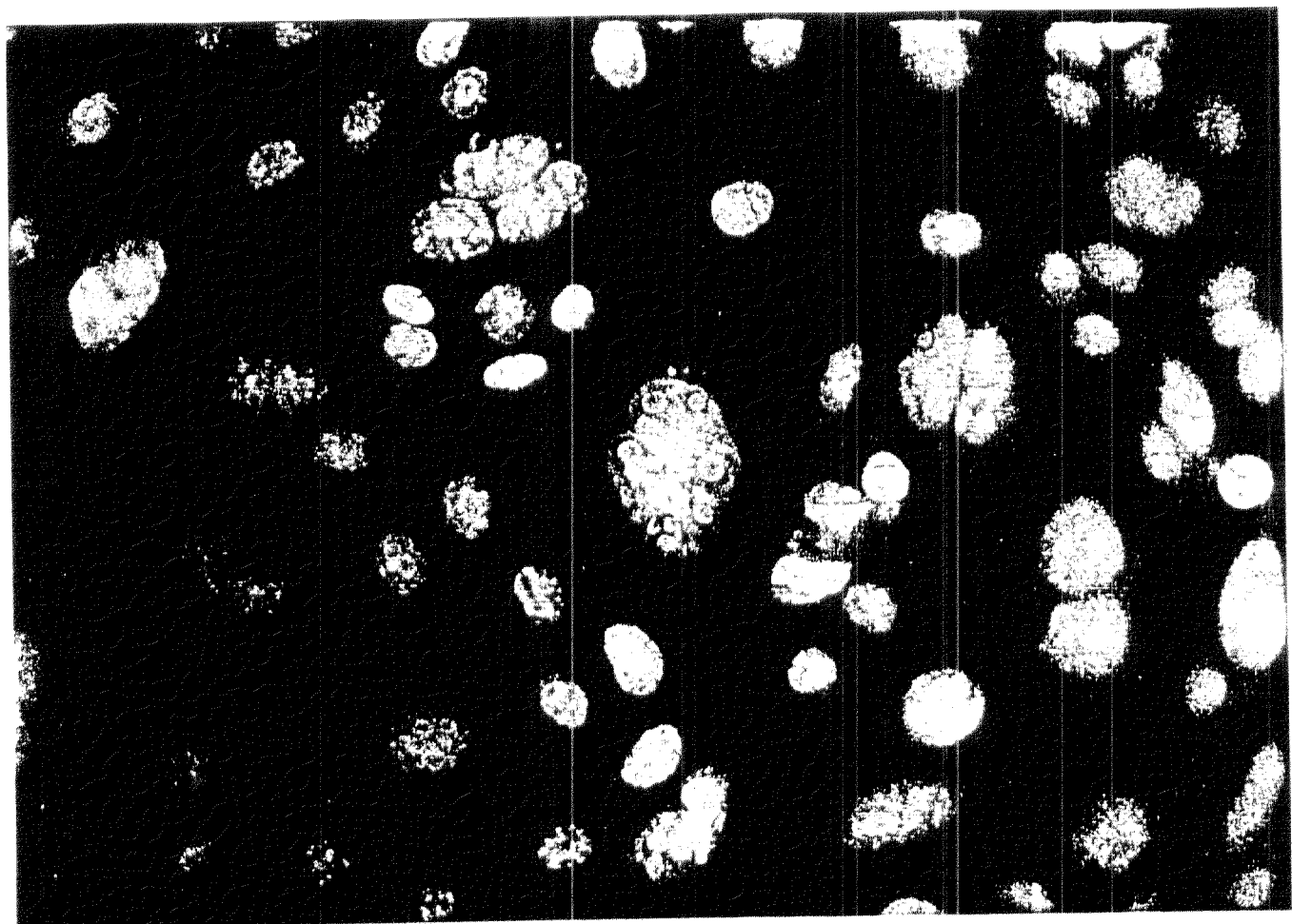
34

Fig. 13. A-B. CHO-K1 cells exposed to alpha-quartz, 30  $\mu\text{g}/\text{sq. cm}$ . A.: Fluorescent light. B: PCOM. X400.



35

Fig. 14. A-B. CHO-K1 cells exposed to UICC Crocidolite, 5  $\mu\text{g}/\text{sq.cm}$ . A.: Fluorescent light. B: PCOM. X400.



36

37

**Table I. Test Particulates, Description of Bulk Materials**

Generic Name	Trade Name or ID Number	Supplier	Chem. Composition Supplier	Crystallinity			
				Supplier Information	MTC Analysis		
				Cristobalite	Quartz	Cristobalite	Quartz
Natural DE	Celite 500	Celite	Silica		<3%	none detected	3.98%
Flux Calcined DE	Hyflo Super Cel Celite 513	Celite	Silica	< 60%	<3%	39.59%	1.95%
Cristobalite	Std. Ref. 1879	NBS*	Silica	96%		not done	not done
alpha-Quartz	Std. Ref. 1878	NBS*	Silica		98%	not done	not done

\*U.S. National Bureau of Standards

38

**Table II. Comparison of Effective Concentration-50, EC 50 CHO-K1 Cells**

EC50 is the concentration which reduces cell proliferation to 50% of negative (unexposed) control cultures.

Test Article	Surface Area	Crystallinity %	Avg. Length	% Fibrous*	% longer than 7.5 µm	Particles/µg (x 1,000)	Effective Concentration-50		
							µg/cm <sup>2</sup>	Part./cm <sup>2</sup> (x 1,000)	F. ≥7.5/cm <sup>2</sup> (x 1,000)
s-Nat DE	~20 cu.M./g	<4% Quartz	3.8	38%	11%	514	4	2060	214
s-FC DE	~2 cu.M./g	~40% Cristobalite	5.9	36%	31%	78	11	860	259
a-Quartz	?	>96% Quartz	2.0	6%	0	525	16	8400	0
Cristobalite	?	>96% Cristobalite	4.6	21%	13%	75	25	1880	214
UICC Crocidolite	?	0	1.8	~100%	4%	2400	4	9600	384
Titanium Dioxide	?	0	n/d	n/d	n/d	n/d	26		

\*Fibrous defined as having aspect ratio >/=3.

**Appendix 1. Test Particles, Dimensions**  
 Measured using SEM.

Particulate	Diameter Range μm	Diameter Avg. μm	Diameter Std. Dev.	Length Range μm	Length Avg. μm	Length Std. Dev.	Aspect Ratio**	
							Avg.	% > 3
s-Nat DE*	0.2-5.8	1.3	1.0	0.9-23.3	3.8	3.9	3.65	38%
s-FC DE*	0.4-8.1	2.1	1.5	0.7-20.7	5.9	4.1	3.50	36%
Cristobalite	0.4-7.8	2.1	1.5	0.7-24.7	4.6	3.9	2.28	21%
alpha-Quartz	0.4-5.1	1.1	0.8	0.5- 8.1	2.0	1.4	1.93	6%

\*Dimensions were analyzed after size-selection processing by MTC Fiber Preparation Laboratory.

\*\*Length/Width

## Appendix 2. Particle Dimensions

Approximately 100 particles of each article were measured using SEM.

Intervals		s-Nat. DE	s-FC DE	Cristobalite	a-Quartz
Length, $\mu\text{m}$		Percent	Percent	Percent	Percent
$\geq$	$<$				
0.0	2.5	47	21	31	78
2.5	5.0	32	27	38	18
5.0	7.5	10	21	18	2
7.5	10.0	5	17	1	2
10.0	12.5	2	6	8	
12.5	15.0	1	3	2	
15.0	17.5	1	3	0	
17.5	20.0	0	1	1	
20.0	22.5	0	1	0	
22.5	25.0	2		1	

Diameter, $\mu\text{m}$					
$\geq$	$<$				
0.0	0.5		4		
0.5	1.0	15	18	5	14
1.0	1.5	32	17	23	52
1.5	2.0	25	16	18	25
2.0	2.5	11	15	17	10
2.5	3.0	8	7	11	2
3.0	3.5	3	7	5	3
3.5	4.0	1	5	5	1
4.0	4.5	3	1	5	2
4.5	5.0	0	5	3	
5.0	5.5	0	1	3	
5.5	6.0	0	0	1	
6.0	6.5	2	0	3	
6.5	7.0		1	0	
7.0	7.5		1	0	
7.5	8.0		0	0	
8.0	8.5		1	2	

40

### Appendix 3. In Vitro Tests

Abbreviation	Name/Description
<b>ICP</b>	<b>Inhibition of Cell Proliferation</b>
	Sixty mm culture dishes are seeded with 100,000 cells in 5 ml complete medium (CM). Cells are allowed to settle to the bottom and, if cell type is anchorage-dependent, cells are allowed to attach before test article is added. Test Particulates are added to cultures in one ml complete medium/dish. Negative control cultures receive 1 ml CM/dish. Each exposure group is set up in triplicate. After three days exposure, at 37°C and 5% CO <sub>2</sub> , cells are harvested with 0.05% Trypsin and 0.02% EDTA in Hanks balanced salt solution (Irvine, Santa Ana, CA) and counted using a Coulter counter. Relative proliferation is determined by dividing the number of cells present in each exposed culture by the number of cells present in unexposed cultures.
<b>CFE</b>	<b>Colony Forming Efficiency</b>
	Sixty mm culture dishes are seeded with 200 cells in 5 ml complete medium and exposed as described for ICP above. Each exposure is set up in triplicate. After 5 days exposure, visible colonies appear. Colonies are stained with 0.4% w/v Giemsa in buffered methanol (Sigma, St. Louis, Missouri). Colonies are counted using a stereoscope at low power. CFE is determined by dividing the number of colonies in each exposed culture by the number of colonies in unexposed cultures.
<b>INA</b>	<b>Induction of Nuclear Abnormalities</b>
	Cultures are prepared as described for ICP above. After two days exposure, culture dishes are fixed with methanol/acetic acid (3:1, v/v) and stained with 0.01% Acridine orange (as described in Clark, 1981). Using a microscope fitted with epifluorescence, the percentage of cells containing micronuclei and/or other visible nuclear abnormalities is determined for each culture dish. Visible nuclear abnormalities include multiple nuclei and lobed nuclei.
<b>EAV</b>	<b>Esterase Activity Viability Test</b>
	Cultures are prepared and exposed as described for ICP above. After 3 days exposure, cells are harvested and resuspended in saline. 5(6)-Carboxyfluorescein diacetate (Sigma, St. Louis, Mo.) is added to each of the cell suspensions (5 µl stock / ml of cell suspension; stock is .1% carboxyfluorescein in acetone diluted 1:1 in saline just before use). After 1--30 minutes at room temperature, hemacytometer counts of the cell suspensions are made using both fluorescence and phase contrast optical microscopy (PCOM). Percent viable cells is determined by dividing the number of fluorescing cells (viable cells) by the number of cells visible with PCOM (total cells).

22

**Appendix 4. Esterase Activity Viability, CHO-K1 Cells.**

Three days exposure to high concentration of test article.  
 Each figure is the average of 4 hemacytometer counts/culture.  
 Data = Cells/Culture Dish, X 10,000.

Test Articles	Concentrtn µg/sq.cm.	Total Cells/Culture Test No.			Fluorescent Cells Test No.			Percent Viable Test No.			Relative Prolif. (% of Control) Avg.	
		#1.	#2.	#3.	#1.	#2.	#3.	#1.	#2.	#3.		
Neg Control	0	317	376	458	316	370	446	100	98	97	98	100
s-Nat DE	20	35	34	43	28	29	35	80	87	81	83	11
s-FC DE	20	89	89	59	83	83	54	94	94	92	93	18
Cristobalite	50	53	103	55	48	87	51	91	84	93	89	18
a-Quartz	50	76			74			97			97	24
Crocidolite	20		22	24		18	20		80	83	81	6

**Appendix 5. Induction of Nuclear Abnormalities**  
Averages from two separate tests.

Fiber	Concentration µg/sq.cm.	Percent w. Mncls.* ± Std. Dev.	Percent Polynuc.** ± Std. Dev.	Percent Abnormal ± Std. Dev.
Control	0	2 ± 1	1 ± 1	3 ± 2
s-Nat DE	3	4 ± 1	8 ± 5	11 ± 6
	5	5 ± 1	11 ± 8	15 ± 7
	10	5 ± 2	19 ± 11	23 ± 9
s-FC DE	20	10 ± 5	23 ± 10	32 ± 4
	5	5 ± 0	10 ± 4	13 ± 4
	10	6 ± 1	14 ± 4	19 ± 5
Cristobalite	20	8 ± 2	23 ± 4	27 ± 3
	30	9 ± 1	32 ± 10	36 ± 7
	5	4 ± 1	5 ± 0	9 ± 0
alpha-Quartz	10	6 ± 1	6 ± 2	12 ± 4
	20	6 ± 2	9 ± 3	14 ± 1
	30	7 ± 3	12 ± 1	18 ± 3
alpha-Quartz	5	4 ± 0	3 ± 1	7 ± 1
	10	7 ± 0	6 ± 0	12 ± 1
	20	4 ± 1	6 ± 2	9 ± 1
30	6 ± 2	6 ± 1	11 ± 2	

\* with one or more micronuclei.  
\*\*with two or more normal-size nuclei; may also have micronuclei.

43